

# The Application of the Sinc-Collocation Approach Based on Derivative Interpolation in Numerical Oceanography

Yasaman Mohseniahouei, Kenzu Abdella, Marco Pollanen

*Department of Mathematics  
Trent University  
Peterborough, Ontario, Canada K9J 7B8*

---

## Abstract

In this paper, the application of a Sinc-Collocation approach based on first derivative interpolation in numerical oceanography is presented. The specific model of interest involves a hydrodynamic model of wind-driven currents in coastal regions and semi-enclosed seas with depth-dependent vertical eddy viscosity. The model is formulated in two different but equivalent systems; a complex-velocity system and a real-valued coupled system. Even in the presence of singularities that are often present in oceanographic problems involving boundary layers, the Sinc-collocation technique provides exponentially convergent approximations. Moreover, the first derivative interpolation approach which uses Sinc-based integration to approximate the unknown has advantages over the customary Sinc method of interpolating the unknown itself since integration has the effect of damping out numerical errors that are inherently present in numerical approximations. Moreover, the approach presented in this paper preserves the appropriate endpoints behaviors of the Sinc bases, resulting in a highly accurate and computationally efficient method. The accuracy and stability of the proposed method is demonstrated through the solution of several model problems. It is further shown that the proposed approach is more accurate and computationally less expensive than those obtained by the Sinc-Galerkin approach reported in previous studies.

*Keywords:* Boundary Value Problems, Ordinary Differential Equations, Sinc Numerical Methods, Wind-Driven Currents, Numerical Oceanography

---

## 1. Introduction

Since the pioneering work of Ekman in 1905, the hydrodynamic problem of wind-driven current systems have been receiving great attention [13]. While Ekman's model was a one-dimensional vertical model, many two and three dimensional systems were later developed [15, 16]. These models are often represented by boundary value problems (BVPs) for which analytic solutions are not available. Therefore, numerical methods including spectral techniques [20], B-spline approach [8], Chebyshev and Legendre polynomials [9] and eigenfunction approach [7] have been applied to obtain

approximate solutions of these BVPs. More Recently, the Sinc-Galerkin method was employed to the wind-driven current model that is considered in this paper [19, 36].

Due to the boundary layer formed by the large magnitude of near-surface velocity shears that is present in these models, traditional numerical methods such as finite-difference methods [25] are not able to resolve the physical processes represented in the models. However, numerical methods based on the Sinc bases are particularly well-suited to these types of Oceanographic problems involving boundary layers since singularities are naturally handled with the Sinc approach. Moreover, Sinc based approximations can be used to approximate the solutions of BVPs over infinite and semi-infinite domains [33] which commonly arise in numerical oceanography. More importantly, they are also

---

\*Corresponding author: Dr. Kenzu Abdella  
Email address: [kabdella@trentu.ca](mailto:kabdella@trentu.ca) (Kenzu Abdella)

characterized by exponentially decaying errors and rapidly converging solutions that can provide highly accurate solutions [5, 6, 11, 12, 17, 30]. Therefore, Sinc-based methods have been applied to diverse scientific and engineering problems including in heat conduction [22, 24, 31], fluid mechanics [27, 28], atomic physics [10, 29], population growth [3], inverse problems [23, 32], astrophysics problems [14, 26], medical imaging [34], elastoplastic problems [2], and in oceanography models [19, 36].

In this paper, a Sinc-Collocation technique based on first derivative interpolation is used to approximate the solution of a steady state model of wind-driven currents with a depth-dependent eddy viscosity in coastal regions and semi-enclosed seas. Winter et al. [36] formulated this model in terms of a complex-valued ordinary differential equation and solved it using the Sinc-Galerkin approach. Recently, Koonprasert and Bowers [19] developed a block matrix formulation for the Sinc-Galerkin technique and applied it to same model but formulated as a coupled system of ordinary differential equations. The Sinc-Collocation approach used in the current paper is applied to the complex as well as the real-value coupled systems.

Following the Sinc function preliminaries in Section 2, we discuss how the model of interest was formulated in Section 3. Section 4 is dedicated to our numerical solutions for both the complex velocity system and the real-value coupled system. Afterwards, we portray our results in Section 5. In closing, concluding remarks are presented in Section 6.

## 2. Sinc Function Preliminaries

On the real line  $\Re$  the Sinc function is defined as

$$\text{sinc}(x) \equiv \begin{cases} \frac{\sin(\pi x)}{\pi x}, & x \neq 0, \\ 1, & x = 0. \end{cases} \quad (1)$$

If  $f$  is a function defined on  $\Re$ , then for a step-size  $h > 0$  the series

$$C(f, h)(x) \equiv \sum_{k=-\infty}^{\infty} f(kh)S(k, h)(x), \quad (2)$$

where  $S(k, h)(x)$  is the scaled and translated  $k^{\text{th}}$  Sinc function given by

$$S(k, h)(x) = \text{sinc}\left(\frac{x - kh}{h}\right) \quad (3)$$

is called the Whittaker Cardinal expansion of  $f$  whenever the series converges. However, in practice, the infinite series defining these approximations are truncated as

$$C_N(f, h)(x) \equiv \sum_{k=-N}^N S(k, h)(x)f(kh), \quad (4)$$

for a given positive integer  $N$ . Note that  $C_N(f, h)(x)$  defines an interpolation of  $f(x)$  with  $C_N(f, h)(x) = f(x)$  at all the Sinc grid points given by  $x_k = kh$ . For a class of functions which are analytic only on an infinite strip containing the real line and allowing specific growth restrictions, the Sinc interpolations provide approximation that exhibit exponentially decaying absolute errors as established by the theorem subsequent to the following definition [35].

**Definition** Let  $D_d$  denote the infinite strip of width  $2d$  ( $d > 0$ ) in the complex plane:

$$D_d = \left\{ z = x + iy \mid |y| < d < \frac{\pi}{2} \right\}.$$

Then  $B^1(D_d)$  is defined as the class of functions  $f$  that are analytic in  $D_d$  such that

$$N(f, D_d) \equiv \lim_{\epsilon \rightarrow 0} \int_{\partial D_d(\epsilon)} |f(z)| |dz| < \infty$$

where

$$D_d(\epsilon) = \left\{ z = x + iy \mid |x| < \frac{1}{\epsilon}, |y| > d(1 - \epsilon) \right\}.$$

**Theorem** If  $f(x) \in B^1(D_d)$  and decays exponentially for  $x \in \Re$  such that

$$|f(x)| \leq \alpha \exp(-\beta \exp(\gamma |x|)) \text{ for all } x \in \Re$$

where  $\alpha$ ,  $\beta$  and  $\gamma$  are positive constants, then the error of the Sinc approximation is bounded by:

$$\sup_{-\infty \leq x \leq \infty} \left| f(x) - \sum_{k=-N}^N S(k, h)(x)f(kh) \right| \leq CE(h)$$

for some positive constant  $C$  and where

$$E(h) = \exp\left(\frac{-\pi d \gamma N}{\log(\pi d \gamma N / \beta)}\right)$$

and the mesh size  $h$  is taken as:

$$h = \frac{\log(\pi d \gamma N / \beta)}{\gamma N}.$$

In order to construct the approximation over the finite interval  $[a, b]$ , we use the change of variable transformation

$$\xi = \varphi(x) = \frac{1}{\pi} \log \left( \frac{x-a}{b-x} \right)$$

with a corresponding inverse

$$x = \psi(\xi) = \frac{b+a}{2} + \frac{b-a}{2} \tanh \left( \frac{\pi}{2} \sinh(\xi) \right)$$

and  $x_k = \psi(kh)$ , that transfers the interval  $[a, b]$  onto  $\mathfrak{R}$  and apply the above Sinc approximation on  $\mathfrak{R}$  to the transformed function  $f(\psi(\xi))$  so that:

$$f(x) \approx \sum_{k=-N}^N S(k, h)(\varphi(x))f(\psi(kh)), \quad a \leq x \leq b, \quad (5)$$

where  $\varphi(a) = -\infty$  and  $\varphi(b) = \infty$ . Therefore, the corresponding error bound theorem will be as follows:

**Theorem** If  $f(\psi(\xi)) \in B^1(D_d)$  and decays exponentially for  $\xi \in \mathfrak{R}$  such that

$$|f(\psi(\xi))\psi'(\xi)| \leq \alpha \exp(-\beta \exp(\gamma|\xi|)) \text{ for all } \xi \in \mathfrak{R}$$

where  $\alpha$ ,  $\beta$  and  $\gamma$  are positive constants and  $x = \psi(\xi)$  is the inverse of the transformation  $\xi = \varphi(x)$ , then the error of the Sinc approximation is bounded by:

$$\sup_{a \leq x \leq b} \left| f(x) - \sum_{k=-N}^N S(k, h)(\varphi(x))f(\psi(kh)) \right| \leq CE(h)$$

for some positive constant  $C$  and where

$$E(h) = \exp \left( \frac{-\pi d \gamma N}{\log(\pi d \gamma N / \beta)} \right)$$

and the mesh size  $h$  is taken as:

$$h = \frac{\log(\pi d \gamma N / \beta)}{\gamma N}.$$

The typical strategy in using the Sinc method to solve BVPs is to start with the Sinc interpolation of the unknown function and to obtain its first and higher derivatives through successive differentiation in order to transform the BVP into discrete systems. However, this approach has a basic drawback as it is well-known that numerical differentiation process is highly sensitive to numerical errors [4].

Having recognized this difficulty Li and Wu proposed a Sinc-method procedure based on the interpolation of the highest derivative and obtaining

the lower derivatives through successive integration [21]. While this has the advantage of averaging and damping out the numerical errors inherently present in the computation of the derivatives, their approach needs to be modified since there are no boundary conditions for the highest derivative interpolation consistent with the Sinc functions which by construction satisfy the homogeneous Dirichlet boundary conditions. In this paper, we utilize the recent approach of Abdella in which the first derivative is interpolated using the Sinc functions which is then numerically integrated in order to obtain the unknown solution [1]. The second derivative is obtained by differentiation of the interpolated function. Nonhomogeneous boundary conditions are treated by making appropriate transformations which convert them to homogeneous cases as required by the Sinc bases.

We approximate  $u'(x)$  as follows:

$$u'(x) \approx \sum_{k=-N}^N S(k, h)(\varphi(x))u'(x_k), \quad a \leq x < b. \quad (6)$$

Therefore, an approximation to the unknown variable  $u(x)$  can be obtained by integration:

$$u(x) = \int_a^x u'(x) + u(a) = \sum_{k=-N}^N h_k(x)u'(x_k), \quad a \leq x < b \quad (7)$$

where

$$h_k(x) = \int_a^x S(k, h)(\varphi(x))dx. \quad (8)$$

Similarly, an approximation to  $u''(x)$  can be obtained by differentiation:

$$u''(x) = \sum_{k=-N}^N g_k(x)u'(x_k), \quad a \leq x < b \quad (9)$$

where

$$g_k(x) = \frac{dS(k, h)(\varphi(x))}{dx}. \quad (10)$$

Therefore, at the Sinc points  $x_i$  we have the following approximations:

$$u'(x_i) = \sum_{k=-N}^N \delta_{i,k}^{(0)} u'(x_k), \quad (11)$$

$$u(x_i) = \sum_{k=-N}^N h \delta_{i,k}^{(-1)} \frac{u'(x_k)}{\varphi'(x_k)}, \quad (12)$$

$$u''(x_i) = \sum_{k=-N}^N \delta_{i,k}^{(1)} \varphi'(x_i) \frac{u'(x_k)}{h}, \quad (13)$$

where

$$\delta_{i,k}^{(-1)} = \begin{cases} \frac{1}{2} + \int_0^{i-k} \frac{\sin(\pi t)}{\pi t}, & k \neq i, \\ \frac{1}{2}, & k = i, \end{cases} \quad (14)$$

$$\delta_{i,k}^{(0)} = \begin{cases} 0, & k \neq i, \\ 1, & k = i, \end{cases} \quad (15)$$

$$\delta_{i,k}^{(1)} = \begin{cases} \frac{(-1)^{i-k}}{i-k}, & k \neq i, \\ 0, & k = i. \end{cases} \quad (16)$$

### 3. Problem Formulation

Over the last century, physical oceanography has evolved from a descriptive to an explanatory and predictive science. The oceanographic model presented here was developed by Winter et al. [36] describing wind-driven currents in coastal regions and semi-enclosed seas.

The model is constructed in a right-handed coordinate system with the vertical coordinate  $z^*$  directed positive downward from the free surface, and with  $x^*$  and  $y^*$  directed positive northward and eastward, respectively. It is assumed that  $z^*$  changes from 0 to  $D_0 = 100 \text{ m}$ , and the plane at  $z^* = D_0 = 100 \text{ m}$  is an impermeable boundary at the seabed [36]. Several assumptions are made in order to simplify this model. The ocean depth,  $D_0$ , and ocean mass density,  $\rho$ , are assumed constant, and the effects of tides, inertial terms, free surface slope, and variations in atmospheric pressure are neglected [36]. For a better understanding, a schematic form of the model is provided in Figure 1. Assuming  $\tau_w$  as the magnitude of a tangential surface wind stress, the currents are represented by  $\tau(0) = \tau_w (\cos(\chi)\hat{x}^* + \sin(\chi)\hat{y}^*)$  where  $\chi$  is the angle between the positive  $x^*$ -axis and the wind direction and  $\hat{x}^*$  and  $\hat{y}^*$  are unit vectors in the positive direction of  $x^*$ -axis and  $y^*$ -axis, respectively. The horizontal wind-drift current,  $q^*(z^*)$ , is the difference between the total velocity and the geostrophic current and given by  $q^*(z^*) = U^*(z^*)\hat{x}^* + V^*(z^*)\hat{y}^*$ . As well, Internal frictional stresses are parameterized as  $\tau(z^*) = -\rho A_v^*(z^*) \frac{dq^*}{dz^*}$ , where the specified effective vertical eddy viscosity coefficient  $A_v^*(z^*)$

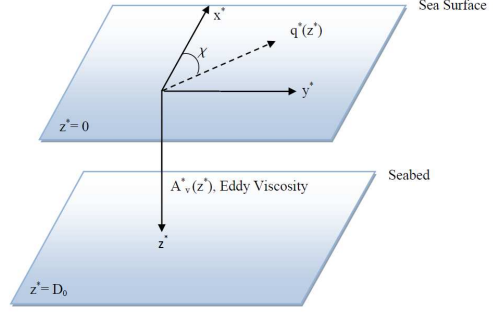


Figure 1: A schematic description of the oceanography model with depth-dependent eddy viscosity

is a continuously differentiable function of  $z^* \in (0, D_0)$  [36]. Therefore, the the wind-drift current,  $q^*$ , is given by the second order differential equation:

$$\frac{d}{dz^*} (A_v^*(z^*) \frac{dq^*}{dz^*}) = -f \hat{z}^* \times q^*, \quad 0 < z^* < D_0, \quad (17)$$

subject to the boundary conditions (BCs)

$$-\rho A_v^*(0) \frac{dq^*(0)}{dz^*} = \tau_w (\cos(\chi)\hat{x}^* + \sin(\chi)\hat{y}^*), \quad (18)$$

$$-\rho A_v^*(D_0) \frac{dq^*(D_0)}{dz^*} = k_f \rho q^*(D_0). \quad (19)$$

The Coriolis parameter at latitude  $\theta$  is given by  $f \equiv 2\Omega \sin(\theta)$ , while  $\Omega = 7.29 \times 10^{-5} \text{ rad s}^{-1}$ . Since the Coriolis force acts inversely in northern and southern hemisphere, Winter et al. [36] assumed that the sea is located in the northern hemisphere, so  $0 < \theta < \frac{\pi}{2}$ . The parameter  $k_f$ , is defined as the linear slip bottom stress coefficient. Substituting the definition of  $q^*(z^*)$  in (17), leads to

$$\begin{aligned} \frac{d}{dz^*} \left( A_v^*(z^*) \frac{dq^*}{dz^*} \right) &= -f \hat{z}^* \times q^* \\ &= -f \hat{z}^* \times [U^*(z^*)\hat{x}^* + V^*(z^*)\hat{y}^*] \\ &= -f (U^*(z^*)\hat{y}^* - V^*(z^*)\hat{x}^*). \end{aligned} \quad (20)$$

which would be separated to its parts as

$$-\frac{d}{dz^*} \left( A_v^*(z^*) \frac{dU^*(z^*)}{dz^*} \right) = -f V^*(z^*), \quad 0 < z^* < D_0, \quad (21)$$

and

$$-\frac{d}{dz^*} \left( A_v^*(z^*) \frac{dV^*(z^*)}{dz^*} \right) = -f U^*(z^*), \quad 0 < z^* < D_0. \quad (22)$$

Similarly, the separated BCs at the sea surface, and the seabed are given by

$$-\rho A^*_v(0) \frac{dU^*(0)}{dz^*} = \tau_w \cos(\chi), \quad (23)$$

$$-\rho A^*_v(0) \frac{dV^*(0)}{dz^*} = \tau_w \sin(\chi),$$

$$\rho A^*_v(D_0) \frac{dU^*(D_0)}{dz^*} = k_f \rho U^*(D_0), \quad (24)$$

$$\rho A^*_v(D_0) \frac{dV^*(D_0)}{dz^*} = k_f \rho V^*(D_0).$$

With the help of the nondimensional variables

$$z \equiv \frac{z^*}{D_0}, \quad A_v(z) \equiv \frac{A^*_v(z^*)}{A^*_v(0)}, \quad (25)$$

$$q(z) \equiv \frac{q^*(z^*)}{U_0} \equiv U(z)\hat{x} + V(z)\hat{y},$$

and nondimensional constants,  $\kappa$  (depth ratio) and  $\sigma$  (bottom friction parameter)

$$\kappa \equiv \frac{D_0}{D_E} = D_0 \sqrt{\frac{f}{2A_0}}, \quad \sigma \equiv \frac{A_0 A_v(1)}{k_f D_0} = \frac{A^*_v(D_0)}{k_f D_0}. \quad (26)$$

where

$$A_0 \equiv A^*_v(0), \quad D_E \equiv \sqrt{\frac{2A_0}{f}},$$

$$U_0 = \frac{\tau_w D_E}{(\rho A_0)} = \frac{\sqrt{2}\tau_w}{(\rho\sqrt{A_0 f})},$$

equations (21) and (22) are transferred to nondimensional equations

$$-\frac{d}{dz} \left( A_v(z) \frac{dU(z)}{dz} \right) = -2\kappa^2 V(z), \quad 0 < z < 1, \quad (27)$$

$$-\frac{d}{dz} \left( A_v(z) \frac{dV(z)}{dz} \right) = 2\kappa^2 U(z), \quad 0 < z < 1. \quad (28)$$

Similarly, the nondimensionalizing procedure on BCs leads to

$$\frac{dU(0)}{dz} = -\kappa \cos(\chi), \quad \frac{dV(0)}{dz} = -\kappa \sin(\chi), \quad (29)$$

$$U(1) + \sigma \frac{dU(1)}{dz} = 0, \quad V(1) + \sigma \frac{dV(1)}{dz} = 0. \quad (30)$$

For the purpose of transforming the nonhomogeneous BCs to homogeneous ones, the following linear transformations are applied.

$$\begin{aligned} U(z) &= u(z) + \kappa(1 + \sigma - z) \cos(\chi), \\ V(z) &= v(z) + \kappa(1 + \sigma - z) \sin(\chi). \end{aligned} \quad (31)$$

The first derivative of the transformations are given by

$$\frac{dU(z)}{dz} = \frac{du(z)}{dz} - \kappa \cos(\chi), \quad (32)$$

$$\frac{dV(z)}{dz} = \frac{dv(z)}{dz} - \kappa \sin(\chi).$$

Hence the ‘‘reduced velocity’’ components  $u(z)$  and  $v(z)$  satisfy

$$-\frac{d}{dz} \left( A_v(z) \frac{du}{dz} \right) + \kappa \cos(\chi) A'_v(z) \quad (33)$$

$$= -2\kappa^2 v(z) - 2\kappa^3(1 + \sigma - z) \sin(\chi), \quad 0 < z < 1,$$

and

$$-\frac{d}{dz} \left( A_v(z) \frac{dv}{dz} \right) + \kappa \sin(\chi) A'_v(z) \quad (34)$$

$$= 2\kappa^2 u(z) + 2\kappa^3(1 + \sigma - z) \cos(\chi), \quad 0 < z < 1.$$

where the BCs at the surface and seabed are respectively given by

$$\frac{du(0)}{dz} = 0, \quad \frac{dv(0)}{dz} = 0, \quad (35)$$

$$u(1) + \sigma \frac{du(1)}{dz} = 0, \quad v(1) + \sigma \frac{dv(1)}{dz} = 0. \quad (36)$$

The system defined by (33)-(36) can be written in two formats; the coupled  $u$  and  $v$  equation systems and complex velocity system. To extract the coupled one, it is assumed that

$$\mathcal{L}u(z) \equiv -\frac{d}{dz} \left( A_v(z) \frac{du}{dz} \right), \quad (37)$$

$$\mathcal{L}v(z) \equiv -\frac{d}{dz} \left( A_v(z) \frac{dv}{dz} \right).$$

Therefore, (33) and (34) will be altered to the coupled  $u$  and  $v$  equation systems

$$\mathcal{L}u(z) + 2\kappa^2 v(z) = F_1(z), \quad 0 < z < 1, \quad (38)$$

$$\mathcal{L}v(z) - 2\kappa^2 u(z) = F_2(z), \quad 0 < z < 1. \quad (39)$$

where

$$F_1(z) = -2\kappa^3(1 + \sigma - z) \sin(\chi) - \kappa \cos(\chi) A'_v(z), \quad (40)$$

$$F_2(z) = 2\kappa^3(1 + \sigma - z) \cos(\chi) - \kappa \sin(\chi) A'_v(z), \quad (41)$$

and BCs at the surface and seabed are respectively given by

$$\frac{du(0)}{dz} = 0, \quad \frac{dv(0)}{dz} = 0, \quad (42)$$

$$u(1) + \sigma \frac{du(1)}{dz} = 0, \quad v(1) + \sigma \frac{dv(1)}{dz} = 0. \quad (43)$$

To obtain the complex velocity formulation, we need to multiply equation (34) by the imaginary unit  $i$ , and add the result to equation (33). In terms of a complex velocity  $w(z) = u(z) + iv(z)$ , we have:

$$\begin{aligned} \mathcal{L}w(z) &\equiv \mathcal{L}u(z) + i\mathcal{L}v(z) \\ &\equiv -\frac{d}{dz} \left( A_v(z) \frac{du(z)}{dz} \right) \\ &\quad - i \frac{d}{dz} \left( A_v(z) \frac{dv(z)}{dz} \right) \\ &\equiv -\frac{d}{dz} \left( A_v(z) \frac{dw(z)}{dz} \right). \end{aligned} \quad (44)$$

Hence the complex velocity formulation is given by

$$\mathcal{L}w(z) - i2\kappa^2 w(z) = F(z), \quad 0 < z < 1, \quad (45)$$

where

$$F(z) = [-\kappa A'_v(z) + i2\kappa^3(1 + \sigma - z)]e^{ix}$$

subject to the boundary conditions given by:

$$w'(0) = 0, \quad (46)$$

$$w(1) + \sigma w'(1) = 0. \quad (47)$$

## 4. Numerical Solutions

In this section, we discuss our treatments to both the complex velocity and coupled systems.

### 4.1. Solution to the Complex Velocity System

The complex velocity problem is given by equations (44)-(47).

As discussed in section 2, we first transform the nonhomogenous BCs to homogeneous ones defining:

$$\eta(z) = w(z) - P(z), \quad (48)$$

where

$$P(z) = w'(0)H_1 + w(0)H_2 + w(1)H_3 + w'(1)H_4, \quad (49)$$

is the univariate Hermite interpolation with the cardinal functions given by:

$$H_1 = z(z-1)^2, \quad H_2 = (z-1)^2(2z+1),$$

$$H_3 = -z^2(2z-3), \quad H_4 = (z-1)z^2.$$

Employing (48) and considering

$$P(0) = w(0), \quad P'(0) = w'(0),$$

$$P(1) = w(1), \quad P'(1) = w'(1).$$

leads to a new BVP given by

$$a(z)\eta''(z) + b(z)\eta'(z) + c(z)\eta(z) + \Lambda(z) = F(z), \quad z \in (0, 1), \quad (50)$$

subject to the homogeneous boundary conditions

$$\eta(0) = \eta(1) = 0, \quad (51)$$

$$\eta'(0) = \eta'(1) = 0, \quad (52)$$

where

$$\Lambda(z) = w'(0)\lambda_1(z) + w(0)\lambda_2(z) + w(1)\lambda_3(z) + w'(1)\lambda_4(z),$$

in which

$$\lambda_1(z) = a(z)H_1'' + b(z)H_1' + c(z)H_1,$$

$$\lambda_2(z) = a(z)H_2'' + b(z)H_2' + c(z)H_2,$$

$$\lambda_3(z) = a(z)H_3'' + b(z)H_3' + c(z)H_3,$$

$$\lambda_4(z) = a(z)H_4'' + b(z)H_4' + c(z)H_4,$$

$$a(z) = -A_v(z), \quad b(z) = -A'_v(z), \quad \text{and} \quad c(z) = -2\kappa^2 i.$$

Now we substitute  $\eta''(z)$ ,  $\eta'(z)$ , and  $\eta(z)$  in equation (50) with those given in (13), (11) and (12) respectively. Therefore, the discretized version of equation (50) will be:

$$\sum_{k=-N}^N M_{i,k} \eta'(z_k) + \Lambda(z_i) = F(z_i), \quad i = -N, \dots, N. \quad (53)$$

where

$$M_{i,k} = a(z_i)\delta_{k,i}^{(1)} \frac{\varphi'(z_i)}{h} + b(z_i)\delta_{k,i}^{(0)} + c(z_i)h \frac{\delta_{k,i}^{(-1)}}{\varphi'(z_k)}. \quad (54)$$

Note that equation (53) leads to a system of  $(2N + 1)$  linear equations for  $(2N + 5)$  unknowns including  $w'(0)$ ,  $w(0)$ ,  $w'(1)$ ,  $w(1)$  and  $\eta'(z_i)$ ,  $i = -N, \dots, N$ .

We define the  $(2N + 5) \times 1$  vector  $\mathbf{C}$  by:

$$\begin{aligned} \mathbf{C} &= [C_{-N-2}, \dots, C_0, \dots, C_{N+2}]^T \\ &= [w(0), w'(0), \eta'(z_{-N}), \dots, \eta'(z_N), w'(1), w(1)]^T. \end{aligned}$$

Two of the four extra conditions required to close the system are obtained from equations (46) and (47):

$$C_{-N-1} = 0, \quad (55)$$

$$C_{N+2} + \sigma C_{N+1} = 0, \quad (56)$$

and the other two from the assumption that  $w$  vanishes at the  $N + 1$  and  $-N - 1$  nodal points:

$$\sum_{k=-N}^N h \delta_{-N-1,k}^{(-1)} \frac{C_k}{\phi'(z_k)} = 0, \quad (57)$$

$$\sum_{k=-N}^N h \delta_{N+1,k}^{(-1)} \frac{C_k}{\phi'(z_k)} = 0. \quad (58)$$

The matrix representation of the  $(2N+5) \times (2N+5)$  system corresponding to equations (53) and (55)-(58) is given by

$$\mathbf{A}\mathbf{C} = \mathbf{F} \quad (59)$$

where  $\mathbf{F}$  is a  $(2N+5) \times 1$  vector given by

$$\mathbf{F} = [0, 0, F(z_N), \dots, F(z_0), \dots, F(z_N), 0, 0]^T,$$

and  $\mathbf{A}$  is a  $(2N+5) \times (2N+5)$  matrix given by

$$\mathbf{A} = \begin{pmatrix} B_1 \\ B_2 \\ \mathbf{B} \\ B_3 \\ B_4 \end{pmatrix}, \quad (60)$$

in which  $B_1, B_2, B_3$  and  $B_4$  are  $1 \times (2N+5)$  matrices given by

$$B_1 = [0, 1, 0, \dots, 0],$$

$$B_2 = [0, 0, \dots, \sigma, 1],$$

$$B_3 = [0, 0, \frac{h\delta_{-N-1,-N}^{(-1)}}{\phi'(z_k)}, \dots, \frac{h\delta_{-N-1,N}^{(-1)}}{\phi'(z_k)}, 0, 0],$$

$$B_4 = [0, 0, \frac{h\delta_{N+1,-N}^{(-1)}}{\phi'(z_k)}, \dots, \frac{h\delta_{N+1,N}^{(-1)}}{\phi'(z_k)}, 0, 0],$$

and  $\mathbf{B}$  as a  $(2N+1) \times (2N+5)$  matrix is given by

$$\mathbf{B} = [\Lambda_2^T, \Lambda_1^T, \mathbf{M}, \Lambda_4^T, \Lambda_3^T],$$

where  $\mathbf{M}$  is the  $(2N+1) \times (2N+1)$  matrix format of (54) and

$$\Lambda_i = [\lambda_i(x_{-N}), \dots, \lambda_i(x_0), \dots, \lambda_i(x_N)].$$

Once equation (59) is solved, the coefficients are used to determine the unknown function  $\eta(z)$  and

$\eta''(z)$  at the Sinc nodes using equations (12) and (13). The original unknown,  $w(z)$  is then determined from equation (48). Note that the values of  $w(z)$  and  $w'(z)$  at the two end-points are also determined directly from the system solutions. The unknowns  $u(z)$  and  $v(z)$  are the real and imaginary parts of  $w(z)$  respectively obtained via

$$u(z) = \text{Re}[w(z)],$$

and

$$v(z) = \text{Im}[w(z)].$$

It should be noted that by construction, the Sinc method is able to handle BVPs involving singularities. Therefore, the linear system arising from the discretization is well posed and do not involve large condition numbers. This was the case for the numerical problems considered in this paper.

#### 4.2. Solution to the Coupled System

The model of interest is also given by the coupled system of differential equations given by equations (37)-(43).

In order to apply our Sinc-Collocation approach to the coupled system, we first transform the boundary value problem as follows:

$$y_u(z) = u(z) - P_u(z), \quad (61)$$

$$y_v(z) = v(z) - P_v(z), \quad (62)$$

where  $P_u(z)$  and  $P_v(z)$  are defined by

$$P_u(z) = u'(0)H_1 + u(0)H_2 + u(1)H_3 + u'(1)H_4,$$

and

$$P_v(z) = v'(0)H_1 + v(0)H_2 + v(1)H_3 + v'(1)H_4.$$

Employing (61), (62) and considering

$$P_u(0) = u(0), \quad P'_u(0) = u'(0),$$

$$P_u(1) = u(1), \quad P'_u(1) = u'(1),$$

$$P_v(0) = v(0), \quad P'_v(0) = v'(0),$$

$$P_v(1) = v(1), \quad P'_v(1) = v'(1).$$

the BVP given by (37)-(43) is transformed into

$$a(z)y_u''(z) + b(z)y_u'(z) + c_1(z)y_v(z) + \Gamma(z) = F_1(z), \quad (63)$$

$$a(z)y_v''(z) + b(z)y_v'(z) + c_2(z)y_u(z) + \Phi(z) = F_2(z), \quad (64)$$

subject to the homogeneous boundary conditions

$$y_u(0) = y_u(1) = 0, \quad y'_u(0) = y'_u(1) = 0,$$

$$y_v(0) = y_v(1) = 0, \quad y'_v(0) = y'_v(1) = 0,$$

where

$$\Gamma(z) = \gamma_1 u'(0) + \gamma_2 u(0) + \gamma_3 u(1) + \gamma_4 u'(1)$$

$$+ \zeta_1 v'(0) + \zeta_2 v(0) + \zeta_3 v(1) + \zeta_4 v'(1),$$

$$\Phi(z) = \gamma_1 v'(0) + \gamma_2 v(0) + \gamma_3 v(1) + \gamma_4 v'(1)$$

$$+ \zeta'_1 u'(0) + \zeta'_2 u(0) + \zeta'_3 u(1) + \zeta'_4 u'(1),$$

in which

$$\gamma_1 = a(z)H''_1 + b(z)H'_1, \quad \gamma_2 = a(z)H''_2 + b(z)H'_2,$$

$$\gamma_3 = a(z)H''_3 + b(z)H'_3, \quad \gamma_4 = a(z)H''_4 + b(z)H'_4,$$

$$\zeta_1 = c_1(z)H_1, \quad \zeta_2 = c_1(z)H_2,$$

$$\zeta_3 = c_1(z)H_3, \quad \zeta_4 = c_1(z)H_4,$$

$$\zeta'_1 = c_2(z)H_1, \quad \zeta'_2 = c_2(z)H_2,$$

$$\zeta'_3 = c_2(z)H_3, \quad \zeta'_4 = c_2(z)H_4.$$

and

$$a(z) = -A_v(z), \quad b(z) = -A'_v(z),$$

$$c_1(z) = 2\kappa^2, \quad c_2(z) = -2\kappa^2,$$

Approximate solutions  $y_u(z)$  and  $y_v(z)$  and their derivatives at the Sinc points  $z_i$  are given by

$$y'_u(z_i) = \sum_{k=-N}^N \delta_{i,k}^{(0)} y'_u(z_k), \quad (65)$$

$$y_u(z_i) = \sum_{k=-N}^N h \delta_{i,k}^{(-1)} \frac{y'_u(z_k)}{\varphi'(z_k)}, \quad (66)$$

$$y''_u(z_i) = \sum_{k=-N}^N \delta_{i,k}^{(1)} \varphi'(z_i) \frac{y'_u(z_k)}{h}, \quad (67)$$

$$y'_v(z_i) = \sum_{k=-N}^N \delta_{i,k}^{(0)} y'_v(z_k), \quad (68)$$

$$y_v(z_i) = \sum_{k=-N}^N h \delta_{i,k}^{(-1)} \frac{y'_v(z_k)}{\varphi'(z_k)}, \quad (69)$$

and

$$y''_v(z_i) = \sum_{k=-N}^N \delta_{i,k}^{(1)} \varphi'(z_i) \frac{y'_v(z_k)}{h}. \quad (70)$$

Therefore, the discretized version of equations (63) and (64) will be given by

$$\sum_{k=-N}^N \left( M_{i,k} y'_u(z_k) + N_{i,k}^1 y'_v(z_k) \right) + \Gamma(z_i) = F_1(z_i), \quad (71)$$

$$\sum_{k=-N}^N \left( M_{i,k} y'_v(z_k) + N_{i,k}^2 y'_u(z_k) \right) + \Phi(z_i) = F_2(z_i), \quad (72)$$

where

$$M_{i,k} = a(z_i) \delta_{k,i}^{(1)} \frac{\varphi'(z_i)}{h} + b(z_i) \delta_{k,i}^{(0)}, \quad (73)$$

$$N_{i,k}^1 = c_1(z_i) h \frac{\delta_{k,i}^{(-1)}}{\varphi'(z_k)}, \quad (74)$$

$$N_{i,k}^2 = c_2(z_i) h \frac{\delta_{k,i}^{(-1)}}{\varphi'(z_k)}. \quad (75)$$

Note that equations (71) and (72) lead to a system of  $(n = 4N + 2)$  equations for  $(m = 4N + 10)$  unknowns.

We define the vector of unknowns  $\mathbf{C}$  by:

$$\mathbf{C} = \mathbf{C}^1 \cup \mathbf{C}^2,$$

where

$$\mathbf{C}^1 = [C_{-N-2}^1, C_{-N-1}^1, \dots, C_0^1, \dots, C_{N+1}^1, C_{N+2}^1]^T$$

$$= [u(a), u'(a), y'_u(x_{-N}), \dots, y'_u(x_N), u'(b), u(b)]^T,$$

and

$$\mathbf{C}^2 = [C_{-N-2}^2, C_{-N-1}^2, \dots, C_0^2, \dots, C_{N+1}^2, C_{N+2}^2]^T$$

$$= [v(a), v'(a), y'_v(x_{-N}), \dots, y'_v(x_N), v'(b), v(b)]^T.$$

The eight more conditions required to close the system consist of

$$C_{-N-1}^1 = 0, \quad (76)$$

$$C_{N+2}^1 + \sigma C_{N+1}^1 = 0, \quad (77)$$

$$\sum_{k=N}^N h \delta_{-N-1,k}^{(-1)} \frac{C_k^1}{\phi'(z_k)} = 0, \quad (78)$$

$$\sum_{k=N}^N h \delta_{N+1,k}^{(-1)} \frac{C_k^1}{\phi'(z_k)} = 0, \quad (79)$$

$$C_{-N-1}^2 = 0, \quad (80)$$

$$C_{N+2}^2 + \sigma C_{N+1}^2 = 0, \quad (81)$$

$$\sum_{k=-N}^N h\delta_{-N-1,k}^{(-1)} \frac{C_k^2}{\phi'(z_k)} = 0, \quad (82)$$

and

$$\sum_{k=N}^N h\delta_{N+1,k}^{(-1)} \frac{C_k^2}{\phi'(z_k)} = 0. \quad (83)$$

Therefore, equations (71), (72), (76)-(83) constitute  $(4N + 10)$  equations for the  $(4N + 10)$  unknowns and can be represented by the matrix equation

$$\mathbf{A}\mathbf{C} = \mathbf{F}, \quad (84)$$

in which  $\mathbf{F}$  is a  $(4N + 10) \times 1$  vector given by

$$\mathbf{F} = \mathbf{F}^1 \cup \mathbf{F}^2,$$

where

$$\mathbf{F}^1 = [0, 0, F_1(z_{-N}), \dots, F_1(z_0), \dots, F_1(z_N), 0, 0]^T,$$

$$\mathbf{F}^2 = [0, 0, F_2(z_{-N}), \dots, F_2(z_0), \dots, F_2(z_N), 0, 0]^T,$$

and  $\mathbf{A}$  is a  $(4N + 10) \times (4N + 10)$  matrix given by

$$A = \left[ \begin{array}{c|c} A^1 & A^2 \\ \hline A^3 & A^4 \end{array} \right],$$

where

$$\mathbf{A}^1 = \begin{pmatrix} B_1 \\ B_2 \\ \mathbf{B} \\ B_3 \\ B_4 \end{pmatrix} \quad (85)$$

where  $B_1, B_2, B_3$  and  $B_4$  are  $1 \times (2N + 5)$  matrices given by

$$B_1 = [0, \sigma, 0, \dots, 0],$$

$$B_2 = [0, 0, \dots, \sigma, 0],$$

$$B_3 = [0, 0, \frac{h\delta_{-N-1,-N}^{(-1)}}{\phi'(z_k)}, \dots, \frac{h\delta_{-N-1,N}^{(-1)}}{\phi'(z_k)}, 0, 0],$$

$$B_4 = [0, 0, \frac{h\delta_{N+1,-N}^{(-1)}}{\phi'(z_k)}, \dots, \frac{h\delta_{N+1,N}^{(-1)}}{\phi'(z_k)}, 0, 0],$$

and  $\mathbf{B}$  is a  $(2N + 1) \times (2N + 5)$  matrix given by

$$\mathbf{B} = [\Gamma_2^T, \Gamma_1^T, \mathbf{M}, \Gamma_4^T, \Gamma_3^T],$$

where  $\mathbf{M}$  is a  $(2N + 1) \times (2N + 1)$  matrix represented by equation (73) and

$$\Gamma_i = [\gamma_i(x_{-N}), \dots, \gamma_i(x_0), \dots, \gamma_i(x_N)].$$

Similarly, the matrix  $A^2$  is a  $(2N + 5) \times (2N + 5)$  matrix given by

$$\mathbf{A}^2 = \begin{pmatrix} \mathbf{0} \\ \mathbf{0} \\ \mathbf{B}^* \\ \mathbf{0} \\ \mathbf{0} \end{pmatrix}, \quad (86)$$

where

$$\mathbf{B}^* = [\Phi_2^T, \Phi_1^T, \mathbf{N}^1, \Phi_4^T, \Phi_3^T],$$

$\mathbf{0} = [0, \dots, 0]$  is a  $(1) \times (2N + 5)$  vector of zeros,  $\mathbf{N}^1$  is a  $(2N + 1) \times (2N + 1)$  matrix represented by equation (75) and

$$\Phi_i = [\zeta_i(x_{-N}), \dots, \zeta_i(x_0), \dots, \zeta_i(x_N)].$$

Note that matrix  $A^4$  is equal to matrix  $A^1$  and matrix  $A^3$  is equal to matrix  $-A^2$ .

Once equation (84) is solved, the coefficients are used to determine the unknown functions  $y_u(z)$  using equations (66) and (69). The original unknowns,  $u(z)$  and  $v(z)$  are then determined from the equations given in (61) and (62). To calculate  $U(z)$  and  $V(z)$  we need to apply equations given in (31).

## 5. Numerical Illustrations

### 5.1. Constant Eddy Viscosity

In this section, we examine the accuracy of the Sinc-Collocation method in the complex velocity system while the eddy viscosity is constant. To make reliable comparisons, all the examples, parameters and variables are same as those carried out in [19, 36].

Since the governing equations and variables were nondimensionalized, the only operative constants in (45)-(47), are  $\kappa = \frac{D_0}{D_E} = 5$ ,  $\sigma = \frac{A^*_v(D_0)}{(k_f D_0)} = 0.1$ , and  $\chi = 45^\circ$  [36]. As well, the nominal values:  $f = 0.0001 \text{ s}^{-1}$ , sea water density  $\rho = 1 \times 10^3 \text{ kgm}^{-3}$ , and air density  $\rho_{air} = 1.25 \text{ kgm}^{-3}$  are adopted. The surface wind stress given by  $\tau_w = C_D \rho_{air} W_w^2$ , is set at 0.1414 in all model problems. The linear slip bottom stress coefficient,  $k_f$  is set at  $0.002 \text{ ms}^{-1}$ .  $A^*_v(0)$  in units of  $\text{m}^2 \text{ s}^{-1}$  is given by

$$A^*_v(0) \approx 0.304 \times 10^{-4} W_w^3 \quad (87)$$

together with the parameters and relationships above, the constant eddy viscosity is chosen to be

$$A^*_v(z^*) \equiv 0.02 \text{ m}^2 \text{ s}^{-1}. \quad (88)$$

In the case of constant eddy viscosity, the exact solution is available and given by  $W^*(z^*) = U_0[U(z) + iV(z)]$  where  $U(z)$  and  $V(z)$  are respectively represented by

$$U(z) = \mathcal{R}(W_c(z)) \cos(\chi) - \mathcal{I}(W_c(z)) \sin(\chi), \quad (89)$$

and

$$V(z) = \mathcal{R}(W_c(z)) \sin(\chi) + \mathcal{I}(W_c(z)) \cos(\chi). \quad (90)$$

$\mathcal{R}(W_c(z))$  and  $\mathcal{I}(W_c(z))$ , refer to the real and imaginary parts of  $W_c(z)$  respectively.  $W_c(z)$  is given by

$$W_c(z) = \frac{\vartheta \sigma \cosh(\Theta) + \sinh(\Theta)}{(1-i)[\cosh(\vartheta) + \vartheta \sigma \sinh(\vartheta)]}, \quad (91)$$

where  $\Theta = \kappa(1-i)(1-z)$  and  $\vartheta = \kappa(1-i)$ .

The results of the Sinc-Collocation approach shown by  $U_c(z_j)$  and  $V_c(z_j)$  were compared with the exact solutions,  $U(z_j)$  and  $V(z_j)$ , at the sinc grid points  $\mathcal{S}$  with the mesh size of

$$h = \frac{\log(\pi d \gamma N / \beta)}{\gamma N}$$

where  $d$ ,  $\gamma$ , and  $\beta$  are equal to  $\frac{\pi}{4}$ , 2, and  $\frac{\pi}{2}$  respectively. In order to provide dimensional representation of the velocities we need to multiply the results by the natural velocity scale  $U_0$ .

To demonstrate the accuracy of the method, the maximum absolute errors are defined by

$$\|E_U\| = \max_{-N-2 \leq j \leq N+2} \{U_0 |U_c(z_j) - U(z_j)|\},$$

$$\|E_V\| = \max_{-N-2 \leq j \leq N+2} \{U_0 |V_c(z_j) - V(z_j)|\},$$

and

$$\|E_W\| = \max\{\|E_U\|, \|E_V\|\}, \quad (92)$$

where the units are  $\text{ms}^{-1}$ .

**Example 1.a.** (seabed linear stress condition in the complex velocity system)

For the purpose of keeping the parameters and variables identical to references [36] and [18], we choose  $\chi = 45^\circ$  and the linear stress condition at the seabed,  $\sigma = \frac{A^* v(D_0)}{(k_f D_0)} = 0.1$ . In this example we solve a discrete system of size  $(2N+5) \times (2N+5)$  given by (59). To demonstrate the numerical convergence of the method we consider  $N = 4, 8, 16, 32$ , and 64. The errors are listed in Table 1 demonstrating a very high degree of accuracy.

In Figure 2 we depict the exponential convergence of the solutions by the horizontal projection

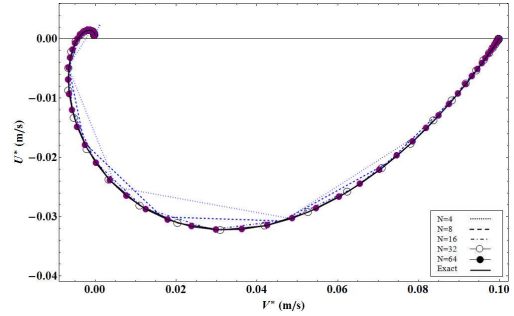


Figure 2: The Sinc-Collocation Ekman Spiral projection of Example 1.a for different values of  $N$  against the exact solution while  $\sigma = 0.1$ ,  $\chi = 45^\circ$ ,  $\kappa = 5$ ,  $D_0 = 100 \text{ m}$ ,  $D_E = 20 \text{ m}$ .

Table 1: Errors of Example 1.a (constant eddy viscosity in the complex system) with  $\sigma = 0.1$ ,  $\chi = 45^\circ$ ,  $\kappa = 5$ ,  $D_0 = 100 \text{ m}$  and  $D_E = 20 \text{ m}$ .

N	h	CPU (s)	$\ E_U\ $	$\ E_V\ $	$\ E_W\ $
4	0.3163	0.015	$2.9852 \times 10^{-3}$	$3.4708 \times 10^{-3}$	$3.4708 \times 10^{-3}$
8	0.2015	0.016	$1.2634 \times 10^{-4}$	$8.4080 \times 10^{-5}$	$1.2634 \times 10^{-4}$
16	0.1224	0.016	$2.4903 \times 10^{-6}$	$1.2267 \times 10^{-6}$	$2.4903 \times 10^{-6}$
32	0.0720	0.125	$2.9558 \times 10^{-8}$	$1.4260 \times 10^{-8}$	$2.9558 \times 10^{-8}$
64	0.0414	0.156	$1.2276 \times 10^{-10}$	$1.817 \times 10^{-10}$	$1.817 \times 10^{-10}$

of the Ekman spiral. Obviously, it is hard to distinguish between the exact solution and the approximate solution while  $N=64$ .

Table 2, provides a comparison between the errors of the Sinc-Collocation method and those in [36] and [18] which are based on the Sinc-Galerkin scheme.  $E_W$ ,  $E_2$  and  $E_3$  convey the maximum errors of our method, and those in [36] and [18] respectively.

**Example 1.b.** (seabed linear stress condition in the coupled system)

We repeat the ideas behind the Example 1.a in the coupled system to check if it is giving us better approximations. In this example we solve a discrete system of size  $(4N+10) \times (4N+10)$  given by (84). Table 3 exhibits the errors of the Sinc-Collocation approach applied to the coupled system. In addition, a comparison between the errors of our method and those in [19] is provided in

Table 2: A comparison between the errors in Example 1.a (in the complex system) and those in papers [18, 36], with  $\sigma = 0.1$ ,  $\chi = 45^\circ$ ,  $\kappa = 5$ ,  $D_0 = 100 \text{ m}$  and  $D_E = 20 \text{ m}$ .

N	h	CPU (s)	$\ E_W\ $	CPU (s)	$\ E_2\ $	$\ E_3\ $
4	0.3163	0.015	$3.4708 \times 10^{-3}$	0.01	$1.10 \times 10^{-3}$	$5.377 \times 10^{-2}$
8	0.2015	0.016	$1.2634 \times 10^{-4}$	0.01	$2.50 \times 10^{-4}$	$4.571 \times 10^{-2}$
16	0.1224	0.016	$2.4903 \times 10^{-6}$	0.03	$2.76 \times 10^{-5}$	$1.861 \times 10^{-2}$
32	0.0720	0.125	$2.9558 \times 10^{-8}$	0.15	$8.99 \times 10^{-7}$	$8.189 \times 10^{-3}$
64	0.0414	0.156	$1.817 \times 10^{-10}$	1.01	$5.78 \times 10^{-9}$	$7.13 \times 10^{-4}$

Table 3: Errors of Example 1.b (constant eddy viscosity in the coupled system) with  $\sigma = 0.1, \chi = 45^\circ, \kappa = 5, D_0 = 100 m$  and  $D_E = 20 m$ .

N	h	CPU (s)	$\ E_U\ $	$\ E_V\ $	$\ E_W\ $
4	0.3163	0.015	$2.9852 \times 10^{-3}$	$3.4708 \times 10^{-3}$	$3.4708 \times 10^{-3}$
8	0.2015	0.016	$1.2634 \times 10^{-4}$	$8.4080 \times 10^{-5}$	$1.2634 \times 10^{-4}$
16	0.1224	0.016	$2.4903 \times 10^{-6}$	$1.2268 \times 10^{-6}$	$2.4903 \times 10^{-6}$
32	0.0720	0.078	$2.9558 \times 10^{-8}$	$1.4260 \times 10^{-8}$	$2.9558 \times 10^{-8}$
64	0.0414	0.109	$7.2213 \times 10^{-11}$	$4.8278 \times 10^{-11}$	$7.2213 \times 10^{-11}$

Table 4: A comparison between the errors in Example 1.b (in the coupled system) and those in paper [19], with  $\sigma = 0.1, \chi = 45^\circ, \kappa = 5, D_0 = 100 m$  and  $D_E = 20 m$ . Here  $m = 2N + 5$  represents the number of unknowns of the linear system.

N	m	h	$\ E_W\ $	$\ E_3\ $
4	13	0.3163	$3.4708 \times 10^{-3}$	$5.377 \times 10^{-2}$
8	21	0.2015	$1.2634 \times 10^{-4}$	$4.571 \times 10^{-2}$
16	37	0.1224	$2.4903 \times 10^{-6}$	$1.861 \times 10^{-2}$
32	69	0.0720	$2.9558 \times 10^{-8}$	$8.189 \times 10^{-3}$
64	133	0.0414	$7.2213 \times 10^{-11}$	$7.13 \times 10^{-4}$

Table 4. The corresponding Ekman spiral to Example 1.b is depicted in Figure 3. Comparing the errors in Tables 1 and 3, shows that the only difference between errors of the complex system and the coupled system happens at  $N = 64$ . At  $N = 64$ , the Sinc-Collocation approach in the coupled system provides more accurate approximation than that in the complex system.

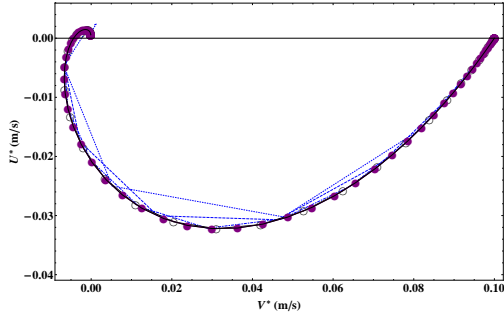


Figure 3: The Sinc-Collocation Ekman Spiral projection of Example 1.b for different values of  $N$  against the exact solution while  $\sigma = 0.1, \chi = 45, \kappa = 5, D_0 = 100 m, D_E = 20 m$ .

### Example 2.a.(No-slip condition at the seabed in the complex velocity system)

In this example we set  $\sigma = 0$ . All other parameters are similar to references [36] and [18] and those carried out in Example 1.a. Here, we solve the discrete system given by (59) for approximate solutions  $U_s(z)$  and  $V_s(z)$ . The errors for different

Table 5: Errors of Example 2.a (constant eddy viscosity in the complex system) with  $\sigma = 0, \chi = 45^\circ, \kappa = 5, D_0 = 100 m$  and  $D_E = 20 m$ .

N	h	CPU (s)	$\ E_U\ $	$\ E_V\ $	$\ E_W\ $
4	0.3163	0.015	$3.0613 \times 10^{-3}$	$3.3831 \times 10^{-3}$	$3.3831 \times 10^{-3}$
8	0.2015	0.016	$1.25 \times 10^{-4}$	$8.4230 \times 10^{-5}$	$1.25 \times 10^{-4}$
16	0.1224	0.016	$2.4824 \times 10^{-6}$	$1.2312 \times 10^{-6}$	$2.4824 \times 10^{-6}$
32	0.0720	0.125	$2.9460 \times 10^{-8}$	$1.4316 \times 10^{-8}$	$2.9460 \times 10^{-8}$
64	0.0414	0.156	$8.2568 \times 10^{-11}$	$8.3657 \times 10^{-11}$	$8.3657 \times 10^{-11}$

Table 6: A comparison between the errors in Example 2.a (in the complex system) and those in [18, 36], with  $\sigma = 0, \chi = 45^\circ, \kappa = 5, D_0 = 100 m$  and  $D_E = 20 m$ .

N	h	CPU (s)	$\ E_W\ $	CPU (s)	$\ E_2\ $	$\ E_3\ $
4	0.3163	0.015	$3.3831 \times 10^{-3}$	0.01	$1.10 \times 10^{-3}$	$5.3322 \times 10^{-2}$
8	0.2015	0.016	$1.25 \times 10^{-4}$	0.01	$2.48 \times 10^{-4}$	$4.5478 \times 10^{-2}$
16	0.1224	0.016	$2.4824 \times 10^{-6}$	0.03	$2.75 \times 10^{-5}$	$1.8543 \times 10^{-2}$
32	0.0720	0.125	$2.9460 \times 10^{-8}$	0.16	$8.96 \times 10^{-7}$	$8.1680 \times 10^{-3}$
64	0.0414	0.156	$8.3657 \times 10^{-11}$	1.07	$5.76 \times 10^{-9}$	$7.1 \times 10^{-4}$

values of  $N$  ( $N=4, 8, \dots, 64$ ) are listed in Table 5 and a very close similarity to those in Example 1.a is explored. The horizontal projection of the Ekman spiral for different values of  $N$  against the exact solution are portrayed in Figure 4. Likewise, Table 6 provides the maximum errors of our method, and those in [36] and [18] respectively.

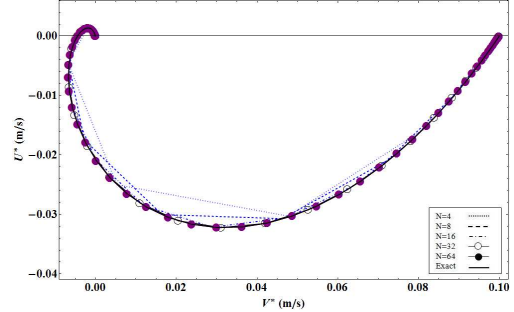


Figure 4: The Sinc-Collocation Ekman Spiral projection of Example 2.a (in the complex system) for different values of  $N$  against the exact solution while  $\sigma = 0, \chi = 45, \kappa = 5, D_0 = 100 m, D_E = 20 m$ .

### Example 2.b.(No-slip condition at the seabed in the coupled system)

Here we repeat the ideas behind Example 2.a in the coupled system to check if there are any differences between the results. Therefore, we solve the system given by (84). Table 7 exhibits the errors of the Sinc-Collocation approach applied to the coupled system. In addition, a comparison between the errors of our method and those in [19] is provided in Table 8. The corresponding Ekman spiral to Example 2.b is depicted in Figure 5. Comparing the

Table 7: Errors of Example 2.b (constant eddy viscosity in the coupled system) with  $\sigma = 0, \chi = 45^\circ, \kappa = 5, D_0 = 100 \text{ m}$  and  $D_E = 20 \text{ m}$ .

N	h	CPU (s)	$\ E_U\ $	$\ E_V\ $	$\ E_W\ $
4	0.3163	0.015	$3.0613 \times 10^{-3}$	$3.3831 \times 10^{-3}$	$3.3831 \times 10^{-3}$
8	0.2015	0.016	$1.25 \times 10^{-4}$	$8.4230 \times 10^{-5}$	$1.25 \times 10^{-4}$
16	0.1224	0.016	$2.4825 \times 10^{-6}$	$1.2312 \times 10^{-6}$	$2.4825 \times 10^{-6}$
32	0.0720	0.078	$2.9460 \times 10^{-8}$	$1.4316 \times 10^{-8}$	$2.9460 \times 10^{-8}$
64	0.0414	0.109	$9.1851 \times 10^{-11}$	$4.4308 \times 10^{-11}$	$9.1851 \times 10^{-11}$

Table 8: A comparison between the errors in Example 2.b (in the coupled system) and those in [19], while  $\sigma = 0, \chi = 45^\circ, \kappa = 5, D_0 = 100 \text{ m}$  and  $D_E = 20 \text{ m}$ .

N	m	h	$\ E_W\ $	$\ E_3\ $
4	13	0.3163	$3.3831 \times 10^{-3}$	$5.3322 \times 10^{-2}$
8	21	0.2015	$1.25 \times 10^{-4}$	$4.5478 \times 10^{-2}$
16	37	0.1224	$2.4824 \times 10^{-6}$	$1.8543 \times 10^{-2}$
32	69	0.0720	$2.9460 \times 10^{-8}$	$8.1680 \times 10^{-3}$
64	133	0.0414	$9.1851 \times 10^{-11}$	$7.1 \times 10^{-4}$

errors in Tables 5 and 7, shows that the only difference between errors of the complex system and the coupled system happens at  $N = 64$ . At  $N = 64$ , the Sinc-Collocation approach in the coupled system provides more accurate approximation than that in the complex system.

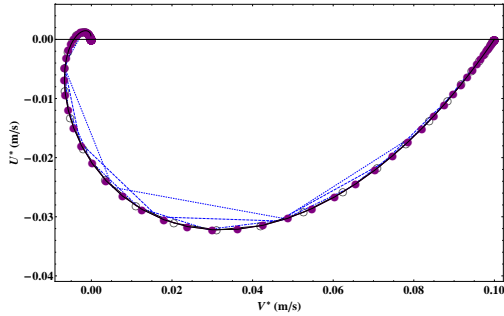


Figure 5: The Sinc-Collocation Ekman Spiral projection of Example 2.b (in the coupled system) for different values of  $N$  against the exact solution while  $\sigma = 0, \chi = 45, \kappa = 5, D_0 = 100 \text{ m}, D_E = 20 \text{ m}$ .

## 5.2. Variable Eddy Viscosity

In the real world the eddy viscosity is a depth- and time-dependent variable. In this paper, we specifically study the depth-dependent eddy viscosity. Likewise, we study a specific case of time-dependent eddy viscosity in which when  $t \rightarrow \infty$ , it can be considered as a constant.

In seas of shallow to intermediate depth, the eddy viscosity has the maximum values of  $A^*_v(z^*)$  at the intermediate depths and the minimum values near

the surface and seabed. But in deeper seas, it is expected that  $A^*_v(z^*)$  has the maximum values near the surface and its value decreases going towards the seabed. The latter case is illustrated by

$$A^*_v(z^*) = 0.02[1 - 0.0075z^*]^2, \quad 0 < z^* < D_0 \quad (93)$$

which decreases quadratically from the value of  $0.02 \text{ m}^2 \text{ s}^{-1}$  to the minimum value of  $0.00125 \text{ m}^2 \text{ s}^{-1}$ . The eddy viscosity in the first case, follows a quadratic model given by

$$A^*_v(z^*) = 0.02[1 + 0.12z^*(1 - 0.01z^*)], \quad 0 < z^* < D_0. \quad (94)$$

increasing from the initial value of  $0.02 \text{ m}^2 \text{ s}^{-1}$  to the peak value of  $0.08$  and then decreasing to  $0.02 \text{ m}^2 \text{ s}^{-1}$ .

**Example 3.a.** (The decreasing eddy viscosity in the complex velocity system)

In this example we find the approximate solutions  $U_s(z)$  and  $V_s(z)$  via the complex velocity discrete system (59), while the variable eddy viscosity is given by (93). The parameters are chosen identical to those in references [36] and [18]. Hence  $D_0 = 100 \text{ m}, \sigma = 0.1, \chi = 45^\circ$ , and  $\kappa = 5$ .

Since there is no closed form solution to the current case, we present the Ekman spiral projection of decreasing eddy viscosity in the complex velocity system against that of constant eddy viscosity for different values of  $N$ , in Figure 6.

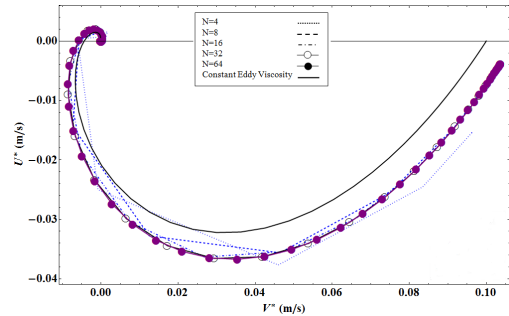


Figure 6: The Sinc-Collocation Ekman Spiral projection of Example 3.a (in the complex system) for different values of  $N$  against the exact solution while  $\sigma = 0.1, \chi = 45, \kappa = 5, D_0 = 100 \text{ m}, D_E = 20 \text{ m}$ .

**Example 3.b.** (The decreasing eddy viscosity in the coupled system)

We applied our approach to the same model problem in Example 3.a but in the coupled system. Again since there is no closed form solution of this

case, we present the results by the Ekman spiral projection of the decreasing eddy viscosity in the coupled system against that of constant eddy viscosity for different values of  $N$ , in Figure 7.

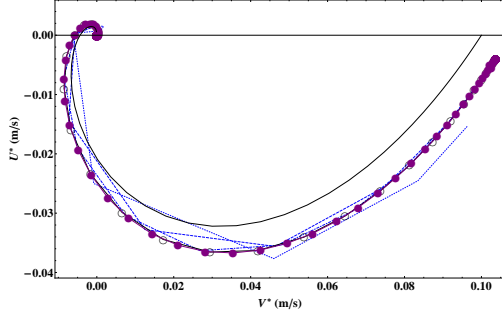


Figure 7: The Sinc-Collocation Ekman Spiral projection of Example 3.b (in the coupled system) for different values of  $N$  against the exact solution while  $\sigma = 0.1$ ,  $\chi = 45$ ,  $\kappa = 5$ ,  $D_0 = 100$  m,  $D_E = 20$  m.

**Example 4.a.** (The quadratic eddy viscosity in the complex velocity system)

In this example, the approximate solutions  $U_s(z)$  and  $V_s(z)$  are demonstrated by the complex velocity discrete system while the eddy viscosity is given by (94). All the parameters are identical to those carried out in Example 1.a. The exact solution of this model problem is not valid. Therefore to discuss the results, we portray the Ekman spiral projection of quadratic eddy viscosity in the complex system against that of constant eddy viscosity for different values of  $N$  by Figure 8.

**Example 4.b.** (The quadratic eddy viscosity in the coupled system)

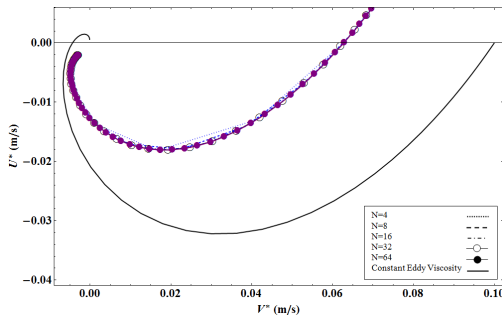


Figure 8: The Sinc-Collocation Ekman Spiral projection of Example 4.a (in the complex system) for different values of  $N$  against the exact solution while  $\sigma = 0.1$ ,  $\chi = 45$ ,  $\kappa = 5$ ,  $D_0 = 100$  m,  $D_E = 20$  m.

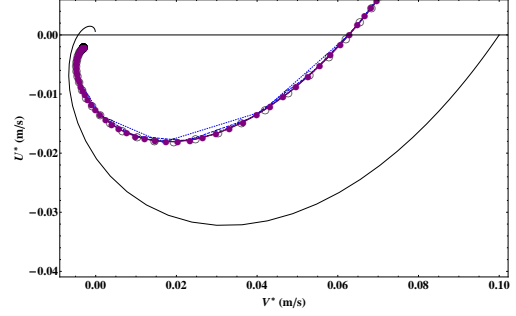


Figure 9: The Sinc-Collocation Ekman Spiral projection of Example 4.b (in the coupled system) for different values of  $N$  against the exact solution while  $\sigma = 0.1$ ,  $\chi = 45$ ,  $\kappa = 5$ ,  $D_0 = 100$  m,  $D_E = 20$  m.

The same model problem as Example 4.a is investigated in the coupled system. Figure 9 shows the results by the help of the Ekman spiral projection of quadratic eddy viscosity in the coupled system against that of constant eddy viscosity for different values of  $N$ .

**Example 5.** (A steady-state problem in the complex system)

As discussed earlier eddy viscosity is a time- and depth-dependent variable. Realistic oceanography problems are those in which eddy viscosity is a function of depth and time. Field studies show that the value of the eddy viscosity near the surface is dependent on the wind stress which relies on time. Therefore, in shallow seas ( $D_0 < 100$  m), the eddy viscosity is assumed dependent of time but independent of depth. There is an interesting example of this case in [18] studied in below.

Assume the nondimensional time-dependent eddy viscosity

$$A_v(t) = 4 - 3e^{-t}.$$

At the steady-state condition ( $t \rightarrow \infty$ ), it will be equivalent to  $A_\infty \equiv 4$ . Then consider the steady-state boundary value problem

$$A_\infty \frac{d^2 w(z)}{dz^2} + 2\kappa^2 i w(z) = -2\kappa^3 i \left( \frac{1-z}{A_\infty} \right) e^{i\chi} \quad (95)$$

with time-independent boundary conditions

$$\frac{dw(0)}{dz} = 0, \quad (96)$$

$$w(1) = 0. \quad (97)$$

and the no-slip boundary condition  $\sigma = 0$ .

Table 9: Errors of Example 5 (the steady-state problem in the complex system) with  $\sigma = 0, \chi = 45^\circ, \kappa = 3.14, D_0 = 60 m$  and  $D_E = 19 m$ .

N	h	CPU (s)	$\ E_U\ $	$\ E_V\ $	$\ E_W\ $
4	0.3163	0.015	$9.6571 \times 10^{-6}$	$3.4867 \times 10^{-6}$	$9.6571 \times 10^{-6}$
8	0.2015	0.015	$4.5835 \times 10^{-8}$	$9.9910 \times 10^{-8}$	$9.9910 \times 10^{-8}$
16	0.1224	0.016	$5.833 \times 10^{-9}$	$2.1325 \times 10^{-9}$	$5.833 \times 10^{-9}$
32	0.0720	0.093	$6.9410 \times 10^{-11}$	$2.5413 \times 10^{-11}$	$6.9410 \times 10^{-11}$
64	0.0414	0.141	$2.4219 \times 10^{-13}$	$3.0335 \times 10^{-13}$	$3.0335 \times 10^{-13}$

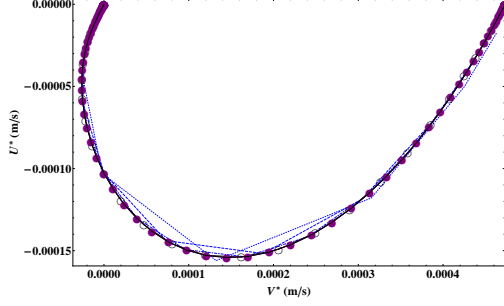


Figure 10: The Sinc-Collocation Ekman Spiral projection of Example 5 for different values of  $N$  against the exact solution while  $\sigma = 0, \chi = 45^\circ, \kappa = 3.14, D_0 = 60 m, D_E = 19 m$ .

The exact solution of this problem is  $W(z) = U_0(U(z) + iV(z))$ , where  $U(z)$  and  $V(z)$  are given by

$$U(z) = R(W_c(z)) \cos(\chi) - I(W_c(z)) \sin(\chi),$$

$$V(z) = R(W_c(z)) \sin(\chi) - I(W_c(z)) \cos(\chi),$$

and

$$W_c(z) = \left( \frac{1+i}{2} \right) \frac{\sinh \left( (1-i)\kappa(1-z) \sqrt{\frac{1}{A_\infty}} \right)}{\sqrt{A_\infty} \cosh \left( (1-i)\kappa \sqrt{\frac{1}{A_\infty}} \right)}. \quad (98)$$

This example is similar to Example 2.a. So we solved the problem by the complex discrete system in (59). The results comparing to the exact solution are depicted in Table 9. Figure 10, displays the Ekman spiral projection of the steady-state problem for  $N = 4, 8, \dots, 64$  against the exact solution. In Table 10, we compare our results with those in [18].

The logarithmic plots of the maximum errors of example 1.a, 2.a and 5 are given by Figures 11, 12 and 13 respectively. These plots show that the errors of our approach decay exponentially.

## 6. Conclusions

In this paper, a Sinc-Collocation technique based on first derivative interpolation has been

Table 10: A comparison between the errors in Example 5 (in the complex system) and those in [18], while  $\sigma = 0, \chi = 45^\circ, \kappa = 3.14, D_0 = 60 m$  and  $D_E = 19 m$ .

N	m	h	$\ E_W\ $	$\ E_3\ $
4	13	0.3163	$9.6571 \times 10^{-6}$	$2.1261 \times 10^{-1}$
8	21	0.2015	$9.9910 \times 10^{-8}$	$2.7372 \times 10^{-1}$
16	37	0.1224	$5.833 \times 10^{-9}$	$8.6065 \times 10^{-2}$
32	69	0.0720	$6.9410 \times 10^{-11}$	$2.2573 \times 10^{-2}$

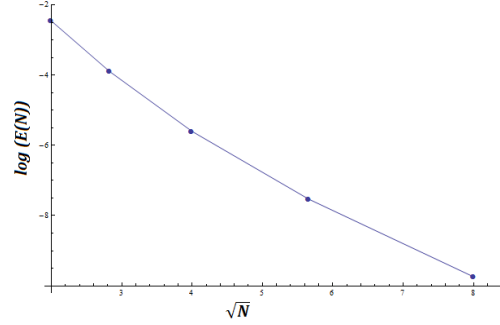


Figure 11: The base-10 logarithm of errors observed in example 1.a versus  $\sqrt{N}$  for  $N=4, 8, 16, 32,$  and  $64$ .

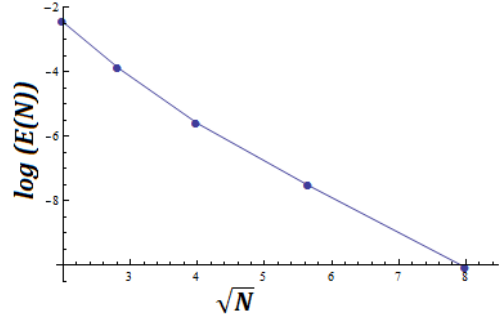


Figure 12: The base-10 logarithm of errors observed in example 2.a versus  $\sqrt{N}$  for  $N=4, 8, 16, 32,$  and  $64$ .

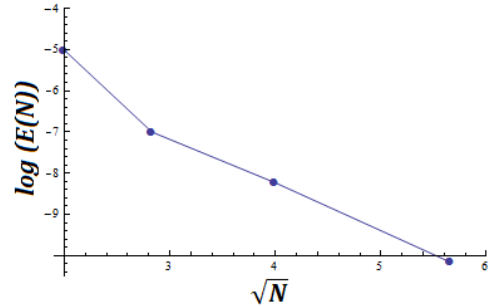


Figure 13: The base-10 logarithm of errors observed in example 5 versus  $\sqrt{N}$  for  $N=4, 8, 16,$  and  $32$ .

used to numerically approximate the solution of a hydrodynamic model observed in [36]. The validity of the proposed approach is demonstrated by solving illustrative examples found in [36] and [19] and comparing the results with the exact solutions and with those in prior studies. The results show that the proposed Sinc-Collocation approach is a computationally efficient and a highly accurate method. In particular, it is shown that the proposed method performs better than the Sinc-Galerkin approach previously used to solve these problems. Therefore, the proposed approach maybe used in numerical oceanography to solve other hydrodynamic problems. Although the focus of this paper is one dimensional oceanography problems, the method utilized in this paper can be extended to solve boundary value problems involving higher dimensions. The extension to higher dimension would follow the approach used in [21].

## Acknowledgements

The general research in Applied Mathematics of one of the authors (KA) is supported by the Natural Sciences and Engineering Research Council of Canada (NSERC).

## References

- [1] K. Abdella. Solving differential equations using sinc-collocation methods with derivative interpolations. *Journal of Computational Methods in Sciences and Engineering*, Submitted, 2014.
- [2] K. Abdella, X. Yu, and I. Kucuk. Application of the sinc method to a dynamic elasto-plastic problem. *Journal of Computational and Applied Mathematics*, 223(2):626–645, 2009.
- [3] Kamel Al-Khaled. Numerical approximations for population growth models. *Applied mathematics and computation*, 160(3):865–873, 2005.
- [4] RL Burden and JD Faires. *Numerical analysis 7th ed.*, brooks/cole, thomson learning, 2001.
- [5] W. Chen, Z.J. Fu, and Qin Q.H. Tboundary particle method with high-order trefftz functions. *Computers Materials and Continua*, 13(3):201–218, 200.
- [6] Wen Chen, Zhuo-Jia Fu, and Ching-Shyang Chen. *Recent Advances in Radial Basis Function Collocation Methods*, volume 2. SpringerVerlag, 2013.
- [7] Alan M Davies. Solution of the 3d linear hydrodynamic equations using an enhanced eigenfunction approach. *International journal for numerical methods in fluids*, 13(2):235–250, 1991.
- [8] AM Davies. The numerical solution of the three-dimensional hydrodynamic equations, using a b-spline representation of the vertical current profile. *Elsevier Oceanography Series*, 19:1–25, 1977.
- [9] AM Davies and A Owen. Three dimensional numerical sea model using the galerkin method with a polynomial basis set. *Applied mathematical modelling*, 3(6):421–428, 1979.
- [10] Mehdi Dehghan and Emami-Naeini Faezeh. The sinc-collocation and sinc-galerkin methods for solving the two-dimensional schrodinger equation with nonhomogeneous boundary conditions. *Applied Mathematical Modelling*, 37(1):9379–9397, 2013.
- [11] Mehdi Dehghan and Abass Saadatmandi. The numerical solution of a nonlinear system of second-order boundary value problems using the sinc-collocation method. *Mathematical and Computer Modelling*, 46(1):1434–1441, 2007.
- [12] Mehdi Dehghan, Mohammad Shakourifar, and Asgar Hamidi. The solution of linear and nonlinear systems of volterra functional equations using adomian-pade technique. *Chaos, Solitons and Fractals*, 39(1):2509–2521, 2009.
- [13] V Walfrid Ekman. On the influence of the earth’s rotation on ocean currents. *Ark. Mat. Astron. Fys.*, 2: 1–53, 1905.
- [14] M El-Gamel and AI Zayed. Sinc-galerkin method for solving nonlinear boundary-value problems. *Computers & Mathematics with Applications*, 48(9):1285–1298, 2004.
- [15] NS Heaps. Three-dimensional model for tides and surges with vertical eddy viscosity prescribed in two layersi. mathematical formulation. *Geophysical Journal of the Royal Astronomical Society*, 64(1):291–302, 1981.
- [16] NS Heaps et al. On the numerical solution of the three-dimensional hydrodynamical equations for tides and storm surges. *Mémoires de la Société Royale des Sciences de Liège. Sixième Série*, 1972.
- [17] Fritz Keinert. Uniform approximation to  $x^\beta$  by sinc functions. *Journal of approximation theory*, 66(1):44–52, 1991.
- [18] Sanoë Koonprasert. *THE SINC-GALERKIN METHOD FOR PROBLEMS*. PhD thesis, MONTANA STATE UNIVERSITY Bozeman, 2003.
- [19] Sanoë Koonprasert and Kenneth L Bowers. Block matrix sinc-galerkin solution of the wind-driven current problem. *Applied mathematics and computation*, 155(3):607–635, 2004.
- [20] RW Lardner and Y Song. A hybrid spectral method for the three-dimensional numerical modelling of nonlinear flows in shallow seas. *Journal of Computational Physics*, 100(2):322–334, 1992.
- [21] Chen Li and Wu Xionghua. Numerical solution of differential equations using sinc method based on the interpolation of the highest derivatives. *Applied Mathematical Modelling*, 31(1):1–9, 2007.
- [22] Andreas Lippke. Analytical solutions and sinc function approximations in thermal conduction with nonlinear heat generation. *Journal of Heat Transfer (Transactions of the ASME (American Society of Mechanical Engineers), Series C);(United States)*, 113(1), 1991.
- [23] John Lund and Curtis R Vogel. A fully-galerkin method for the numerical solution of an inverse problem in a parabolic partial differential equation. *Inverse Problems*, 6(2):205, 1999.
- [24] S. Narasimhan, J. Majdalani, and F. Stenger. A first step in applying the sinc collocation method to the nonlinear navier-stokes equations. *Numerical Heat Transfer: Part B: Fundamentals*, 41(5):447–462, 2002.

- 1  
2  
3  
4 [25] M Aslam Noor and EA Al-Said. Finite-difference  
5 method for a system of third-order boundary-value  
6 problems. *Journal of optimization theory and appli-*  
7 *cations*, 112(3):627–637, 2002.
- 8 [26] K Parand and A Pirkhedri. Sinc-collocation method for  
9 solving astrophysics equations. *New Astronomy*, 15(6):  
10 533–537, 2010.
- 11 [27] K. Parand, Mehdi Dehghan, and A. Pirkhedri. The  
12 use of sinc-collocation method for solving falkner-skan  
13 boundary-layer equation. *International Journal for Nu-*  
14 *merical Methods in Fluids*, 68:36–47, 2007.
- 15 [28] K Parand, Mehdi Dehghan, and A. Pirkhedri. Sinc-  
16 collocation method for solving the blasius equation.  
17 *Physics Letters A*, 373(1):4060–4065, 2009.
- 18 [29] K. Parand, Mehdi Dehghan, and A. Pirkhedri. The  
19 sinc-collocation method for solving the thomas-fermi  
20 equation. *Journal of Computational and Applied Math-*  
21 *ematics*, 237:244–252, 2013.
- 22 [30] Abass Saadatmandi and Mehdi Dehghan. The use of  
23 sinc-collocation method for solving multi-point bound-  
24 ary value problems. *Communications in Nonlinear Sci-*  
25 *ence and Numerical Simulation*, 17(1):593–601, 2012.
- 26 [31] Abass Saadatmandia, Mehdi Dehghan, and  
27 Mohammad-Reza Azizi. The sinc-legendre collocation  
28 method for a class of fractional convection-diffusion  
29 equation with variable coefficients. *Communications*  
30 *in Nonlinear Science and Numerical Simulation*, 17  
31 (1):4125–4136, 2012.
- 32 [32] Ralph C Smith and Kenneth L Bowers. Sinc-galerkin  
33 estimation of diffusivity in parabolic problems. *Inverse*  
34 *problems*, 9(1):113, 1999.
- 35 [33] F. Stenger. Summary of sinc numerical methods. *Jour-*  
36 *nal of Computational and Applied Mathematics*, 121  
37 (1):379–420, 2000.
- 38 [34] Frank Stenger and Michael J O'Reilly. Computing so-  
39 lutions to medical problems via sinc convolution. *Auto-*  
40 *matic Control, IEEE Transactions on*, 43(6):843–848,  
41 1998.
- 42 [35] Masaaki Sugihara and Takayasu Matsuo. Recent de-  
43 velopments of the sinc numerical methods. *Journal of*  
44 *computational and applied mathematics*, 164:673–689,  
45 2004.
- 46 [36] DF Winter, Kenneth L Bowers, and John Lund. Wind-  
47 driven currents in a sea with a variable eddy viscos-  
48 ity calculated via a sinc-galerkin technique. *Internat-*  
49 *ional journal for numerical methods in fluids*, 33(7):  
50 1041–1073, 2000.

## \*Highlights (for review)

- This study uses Sinc-Collocation method based on first derivative interpolation.
- It solves a wind-driven hydrodynamic model with depth-dependent eddy viscosity.
- The scheme is shown to be highly accurate and computationally efficient.
- The validity of the scheme is tested with several model problems.
- The proposed scheme outperforms other schemes based on Sinc approximations.

## Responses to the Reviewers Reports on Manuscript JOCS-D-14-00157

Title: "The Application of the Sinc-Collocation Approach Based on Derivative Interpolation in Numerical Oceanography"

By Yasaman Mohseniahouei, Kenzu Abdella and Marco Pollanen

We want to thank the reviewers for the thorough and constructive review of the paper. We have considered all the comments they raised and made the appropriate changes. The following is a point by point response to the comments made by each referee.

### Reviewer #1:

*The current article investigates on a practical problem and finds the approximate solution of the corresponding differential equation via a numerical technique. The technique is based on Sinc-collocation approach. Several test problems are given and the numerical simulations are reported to observe the efficiency and applicability of the method. The paper is well-written and the results are useful for the interested reader of this computational journal. Thus I recommend its publication, however the following corrections improve the current version.*

#### Response:

We want to thank this reviewer for the positive comments on the manuscript and for recommending it for publication.

- 1- *Can the accuracy of the result be improved via employing Pade approximation or using any other technique?*

#### Response:

To the best of our knowledge no work has been done in terms of the use of Pade approximation to improve the Sinc numerical method. As noted in the current manuscript, there have been a number of improvements made to the standard Sinc method including the use of Double Exponential transformation functions as proposed by Masaaki and Sugihara. Other improvements include the works of Jian Wang (doi:10.1016/j.amc.2007.09.044) and Saadatmandi et al. (Commun Nonlinear Sci Numer Simulat 17 (2012) 4125–4136) who used Legendre polynomials to improve the Sinc-Collocation approach. However, consideration of such improvement in the context of our manuscript is beyond the scope of this paper and would require a separate investigation. We want to thank the reviewer for suggesting this investigation as we plan to include it in our future work.

- 2- *Authors have employed the technique for a one-dimensional model (I mean one-dimension on the space). Discussion on the possibility of developing the idea for higher-dimensional models helps the reader, as it is not easy to apply the classic Sinc method for solving higher-dimensional problems, always.*

#### Response:

This is also a very important comment made by this reviewer. As the reviewer pointed out, the focus of the current manuscript is on one dimension. However, we are already working on extension of the approach to higher dimensional problems. We have added a description of this in the conclusion and added a new reference (Reference [16]) to a paper that has used a similar approach in two dimensions.

- 3- *In page 9, a brief discussion on the condition number of the linear systems arising from the discretization is helpful? Are the corresponding systems well-posed?*

**Response:**

We have added a short description at the end of section 4.1 regarding the linear system arising from the method. By construction, the Sinc method is meant to handle BVPs involving singularities which result in well posed linear systems. We noted that for the numerical problems considered in the paper, there were no numerical difficulties associated with the linear system.

- 4- *Considering the subject of the paper and its discussion, the introduction and literature review of the paper be up-dated by referring to the following research works on the application of Sinc-Collocation:*

**Response:**

We thank the reviewer for pointing out these seven up-dated references. We have now included them into the revised version.

**Reviewer #3:**

*In the present paper, a Sinc-Collocation approach based on first derivative interpolation is presented to analyze a hydrodynamic model. Several examples demonstrate the accuracy and stability of the method. Overall the paper can be accepted if some minor changes are made.*

**Response:**

We want to thank this reviewer for the positive comments on the manuscript and for recommending it for publication.

- 1- *In the introduction, the authors miss some recent related references and need to present the readers big pictures on numerical methods for boundary value problems. Regarding this aspect, I suggest that the revised paper should cite the following papers: (a) Chen, Wen; Fu, Zhuo-Jia; Chen, Ching-Shyang: *Recent Advances in Radial Basis Function Collocation Methods*, SpringerVerlag, 2013. The above book introduces Radial Basis Function Collocation Methods to the solution of boundary value problems. (b) Chen, W., Fu, Z.J., Qin Q.H.: *Boundary particle method with high-order Trefftz functions*. *CMC: Computers, Materials, & Continua*, 13(3), 201-218 (2009). The above paper introduces Trefftz collocation method for solving boundary value problems.*

**Response:**

We thank the reviewer for pointing out these two relevant references. We have now included them into the revised version.

- 2- *It would be better to delete the conclusion of the present method in the introduction, namely, deleting the following sentence "The results presented in this paper demonstrate that the proposed approach is more accurate and computationally less expensive than those obtained by the Sinc-Galerkin approach reported in the previous studies."*

**Response:**

Done.

3- *There are some typos in this paper and the authors should correct all of them.*

**Response:**

We went through the manuscript thoroughly and made a total of 11 typos correction

4- *In page 6, there is an unnecessary number "27" in the first formula.*

**Response:**

This is now fixed.

5- *It would be useful to explain the meaning of  $m$  in Table 4. Is it the number of unknowns?*

**Response:**

Yes  $m$  represents the number of unknowns and is given by  $2N+5$ . This is now explained in the caption of Table 4.

**Reviewer #4:**

*This research presents a new approach in applying the Sinc-Collocation method. Rather than applying the usual Sinc method whereby the unknown function is interpolated, the authors propose to apply the Sinc-Collocation technique to the first derivative and then use Sinc-based integration to obtain the unknown function. The technique is illustrated through a series of oceanographic examples involving wind-driven currents and depth-dependent vertical eddy viscosity. The examples are chosen to be identical to those of previous research for comparison purposes. The results demonstrate that the proposed technique is more accurate and also more computationally efficient than the Sinc-Galerkin method used in previous studies. The Journal of Computational Science is an appropriate journal for this research. My feeling is that this study makes an important and significant contribution to the field, and hence, is worthy of publication provided the following comments are addressed:*

**Response:**

We want to thank this reviewer for the positive comments on the manuscript and for recommending it for publication.

1- *The authors state in the abstract, " ... the first derivative interpolation approach ... has advantages over the customary Sinc method ... since integration has the effect of damping out numerical errors ...". If this is true, then applying the Sinc-Collocation technique to the second derivative should be even more advantageous. Have the authors considered this? Is there a physical explanation if this is not the case? What is the accuracy associated with this approach (for example, is it better than the Sinc-Galerkin method)?*

**Response:**

The paragraph just before equation (6) is now modified and addresses this issue. Our method is more accurate than the Sinc-Galerkin method as shown in the tabulated results which compare the absolute error associated with the current method and that of [14] who used Sink-Galerkin as mentioned in the first paragraph of the Introduction section.

- 2- *In my opinion the paper can be shortened and still make the same impact. For example, in Section 4 equations (47)-(50) are identical to equations (44)-(46) and likewise equations (64)-69) are identical to equations (38)-(43). Why repeat the equations? Also, there are too many examples given in Section 5. The important examples are those that make direct comparisons with previous studies; examples 3b and 4b, for example, offer very little information and can probably be removed.*

**Response:**

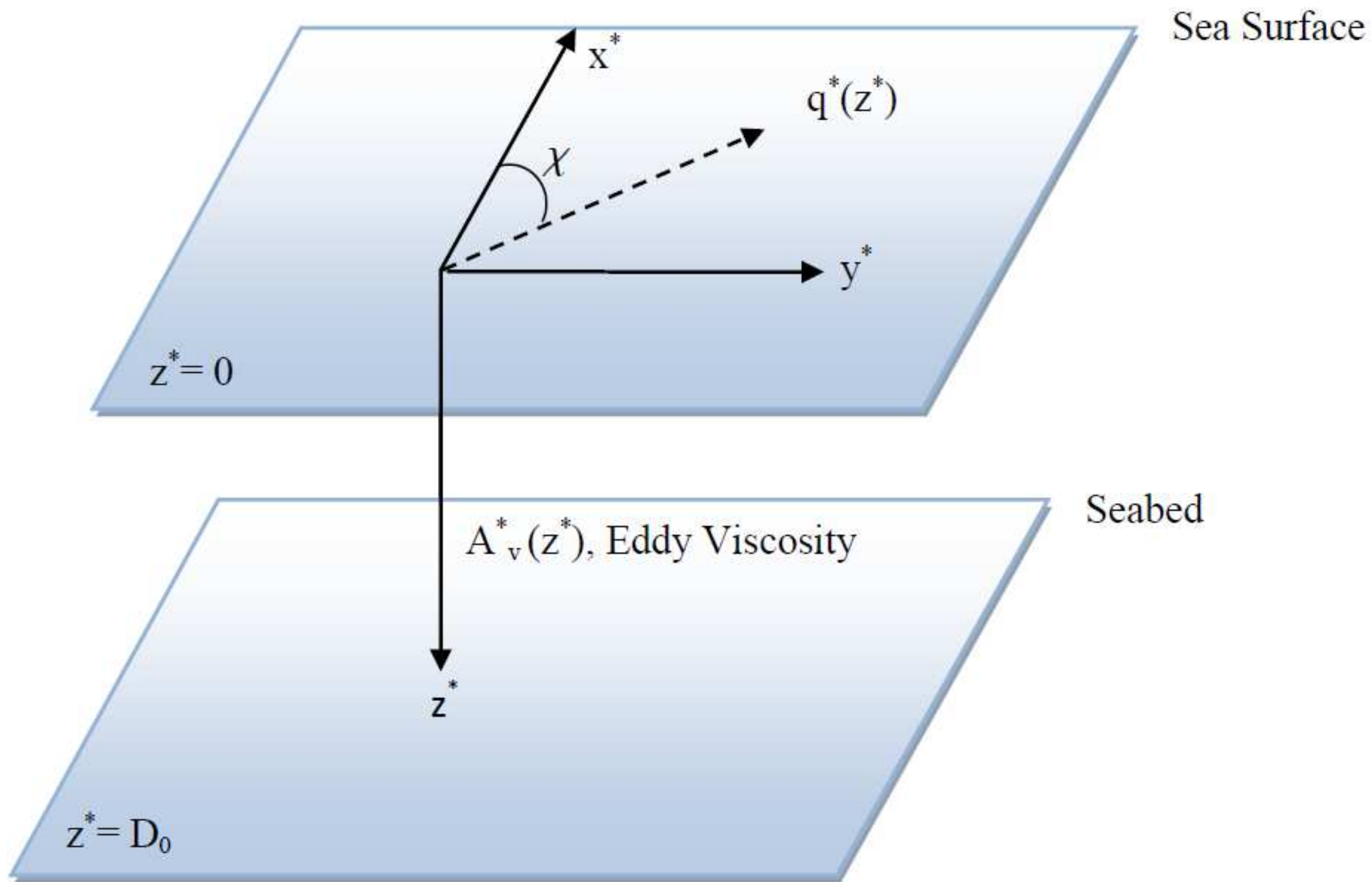
We agree with the reviewer. We have now removed the duplicate equations which were included with the aim of each section self-contained. However, we retained examples 3b and 4b which demonstrate the equivalence of solutions obtained from the coupled and the complex form of the problems.

- 3- *Lastly, the following typos were spotted: Page 1, line 53: "Legender" should be "Legendre" Page 3, equation 5: should it be  $a \leq x \leq b$  instead of  $a \leq x < b$  Page 6, the un-numbered equation above (44) has the number 27 appearing in the middle of the equation.*

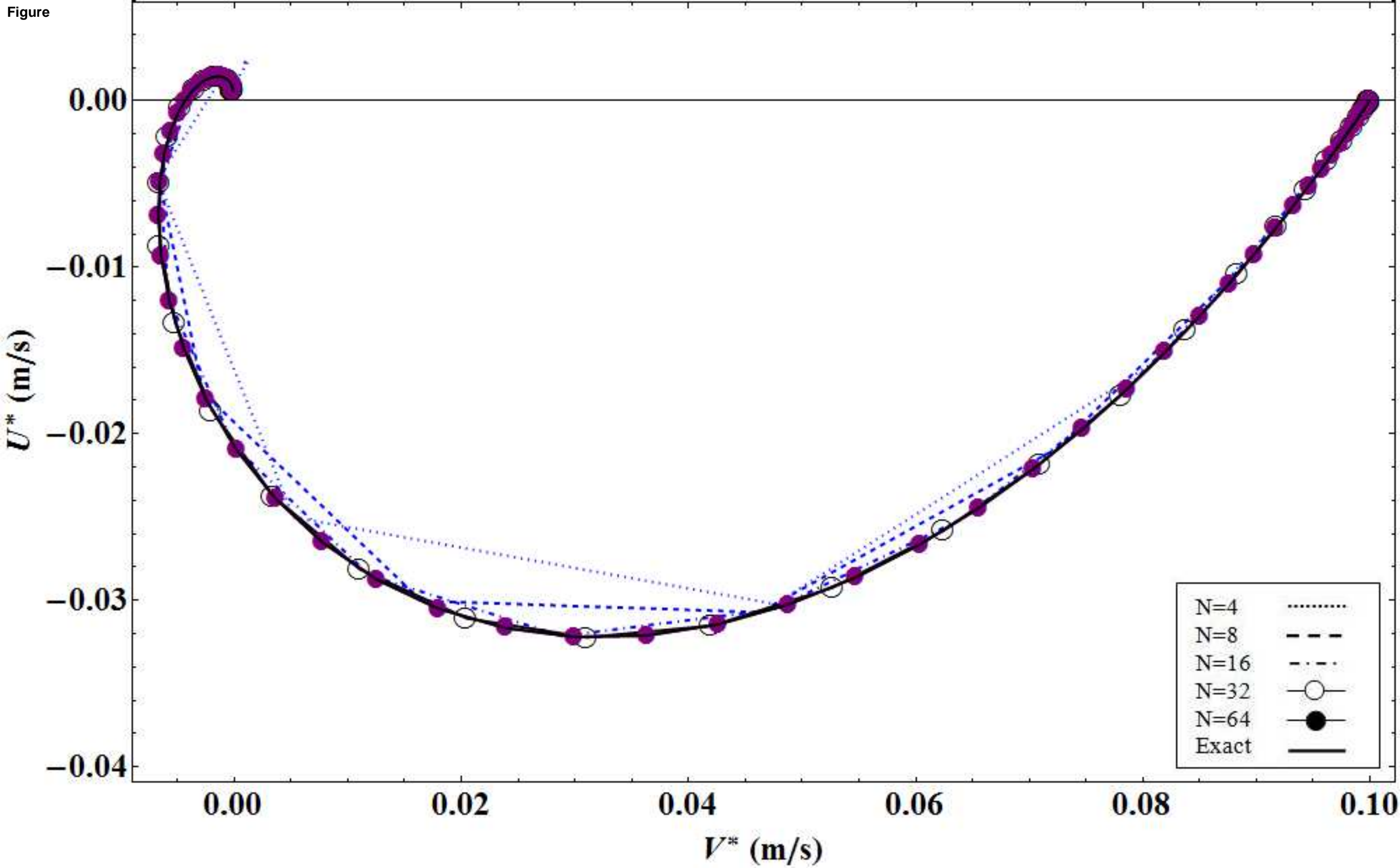
**Response:**

Done.

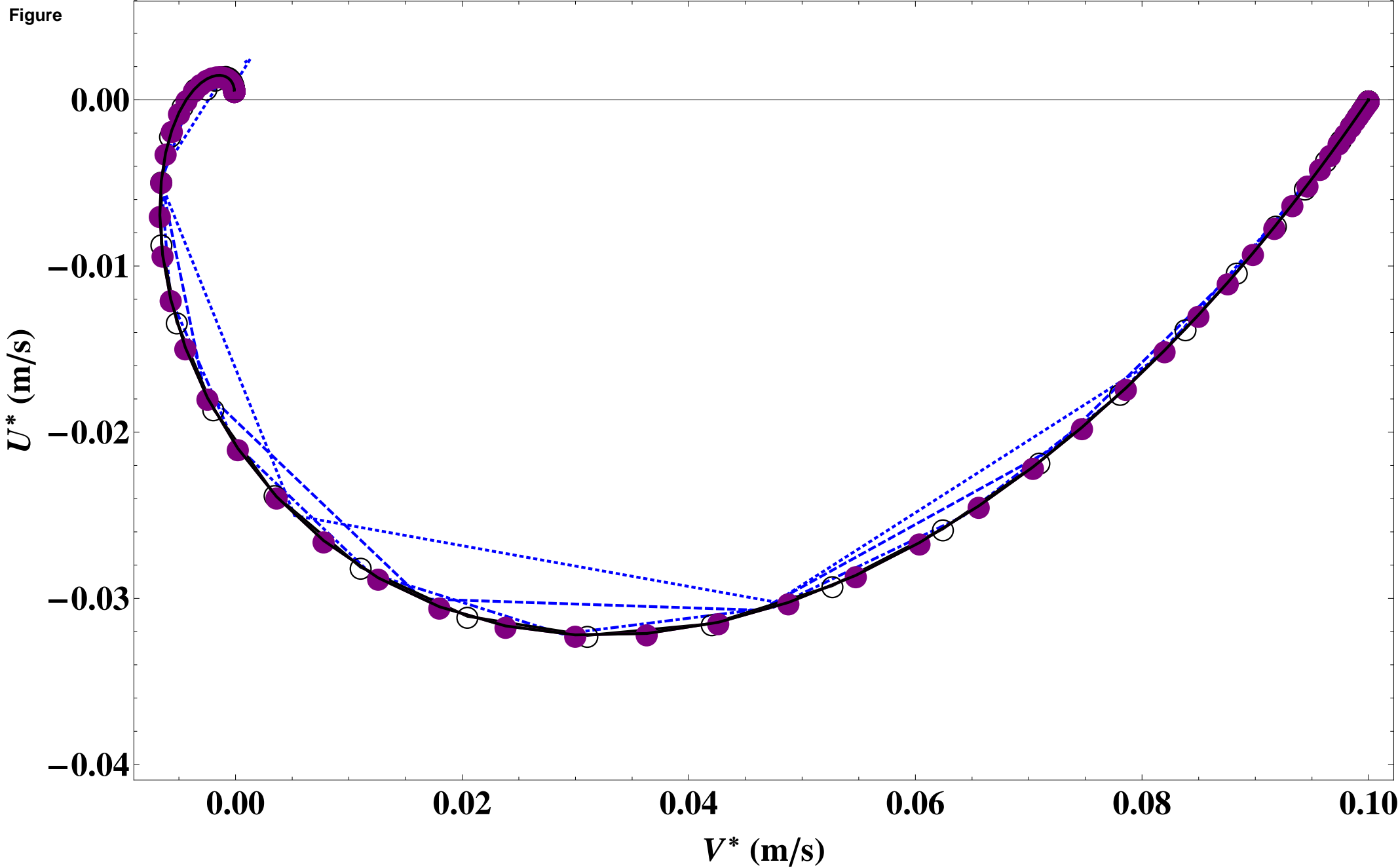
Figure



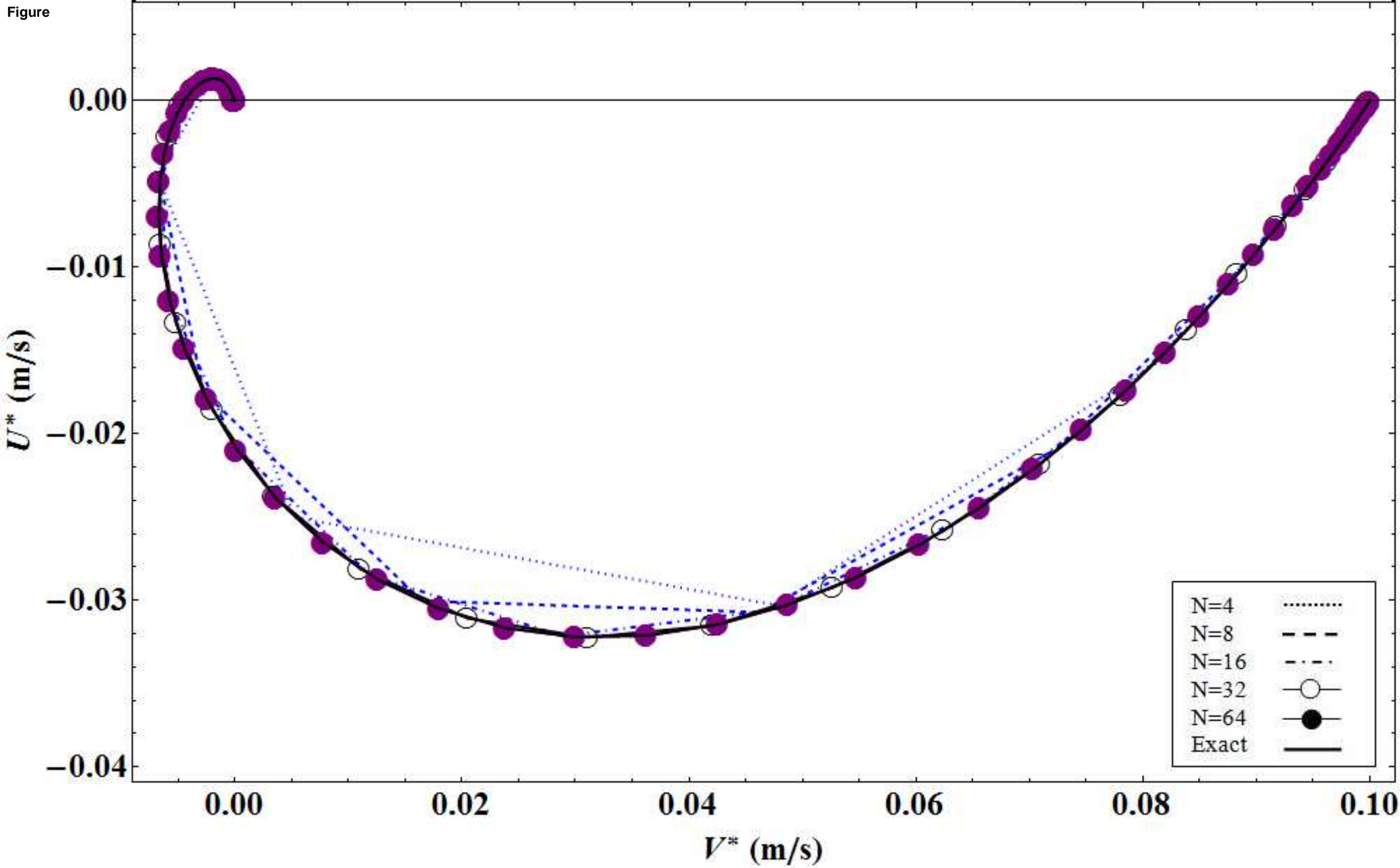
Figure



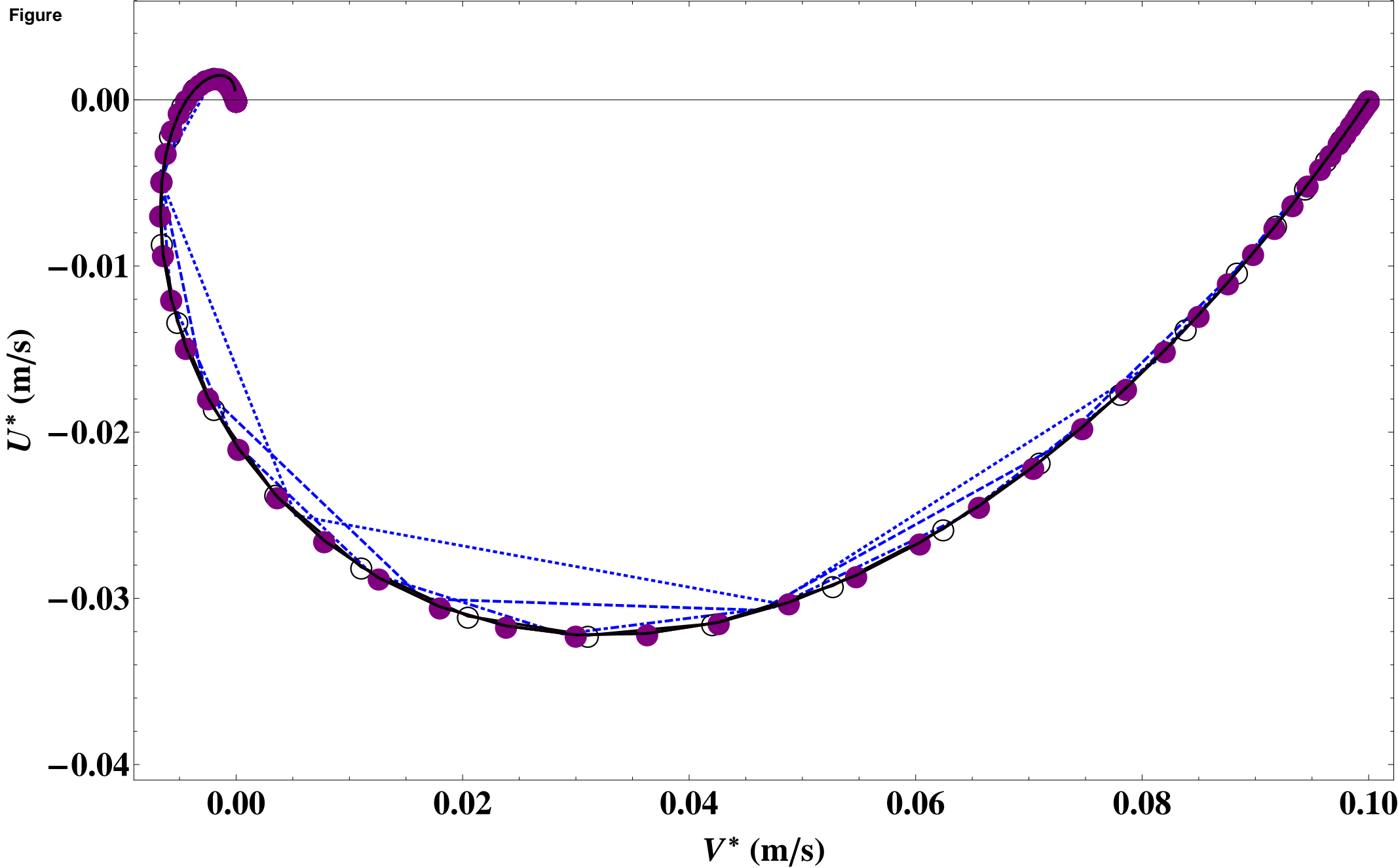
Figure



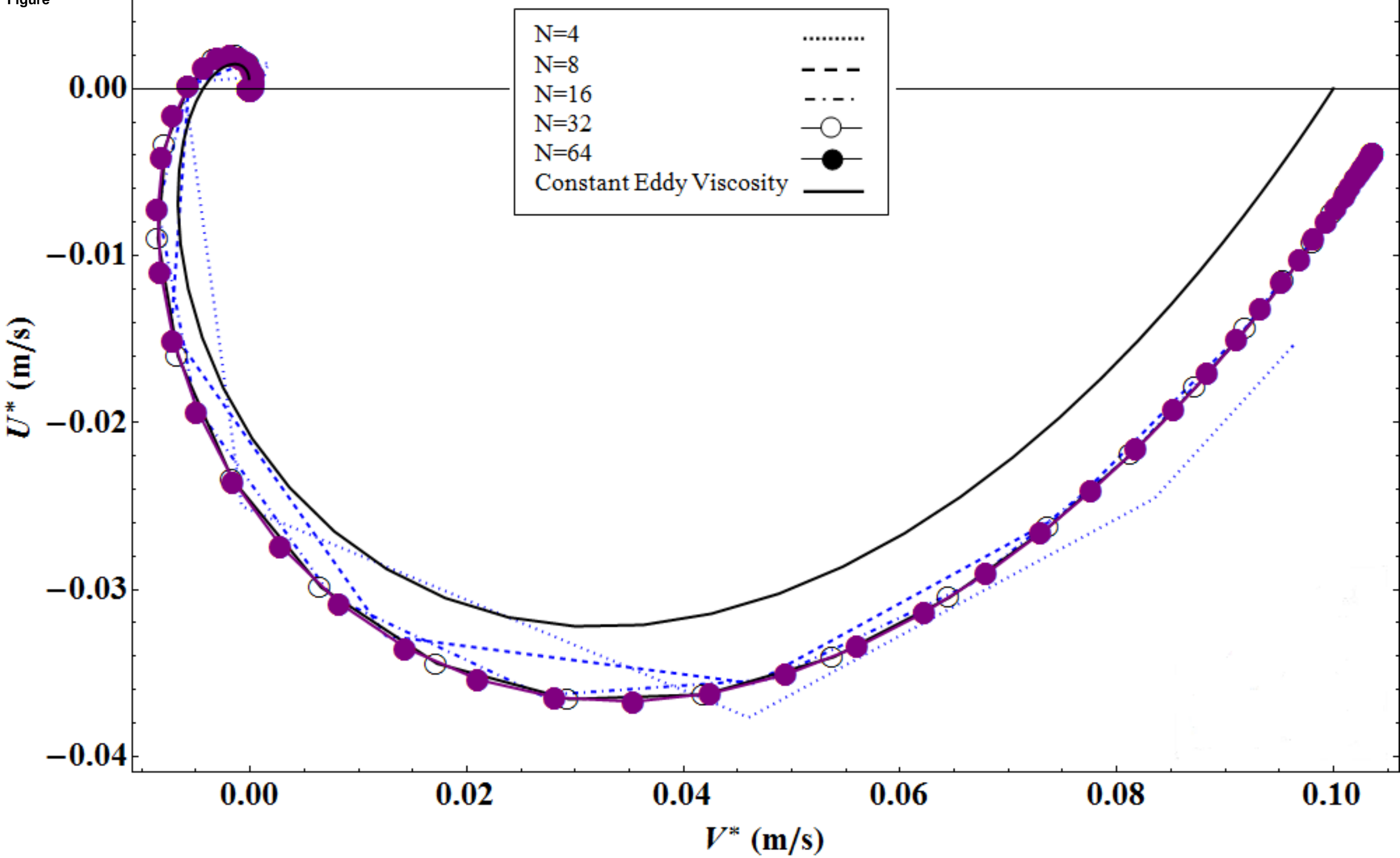
Figure



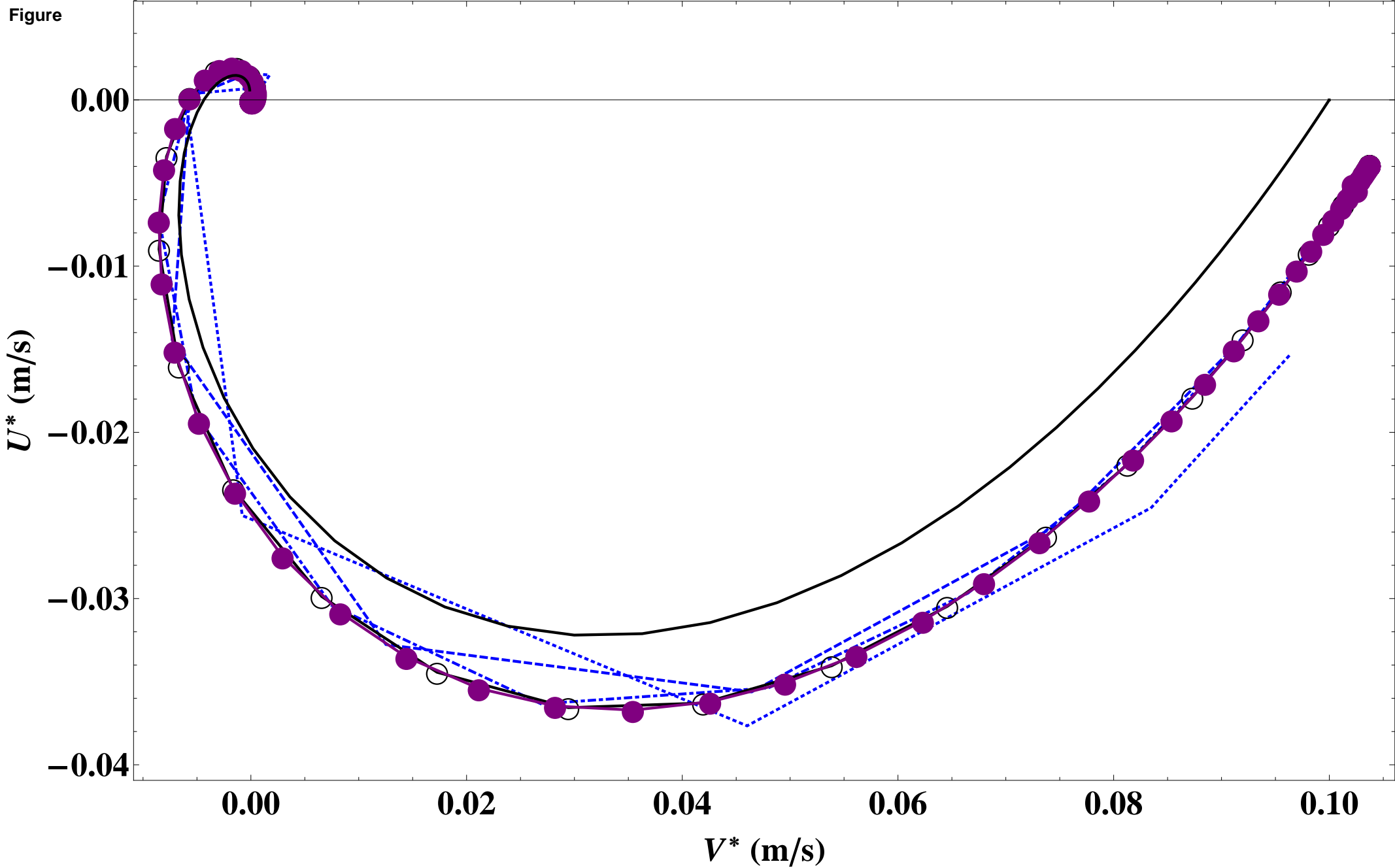
Figure



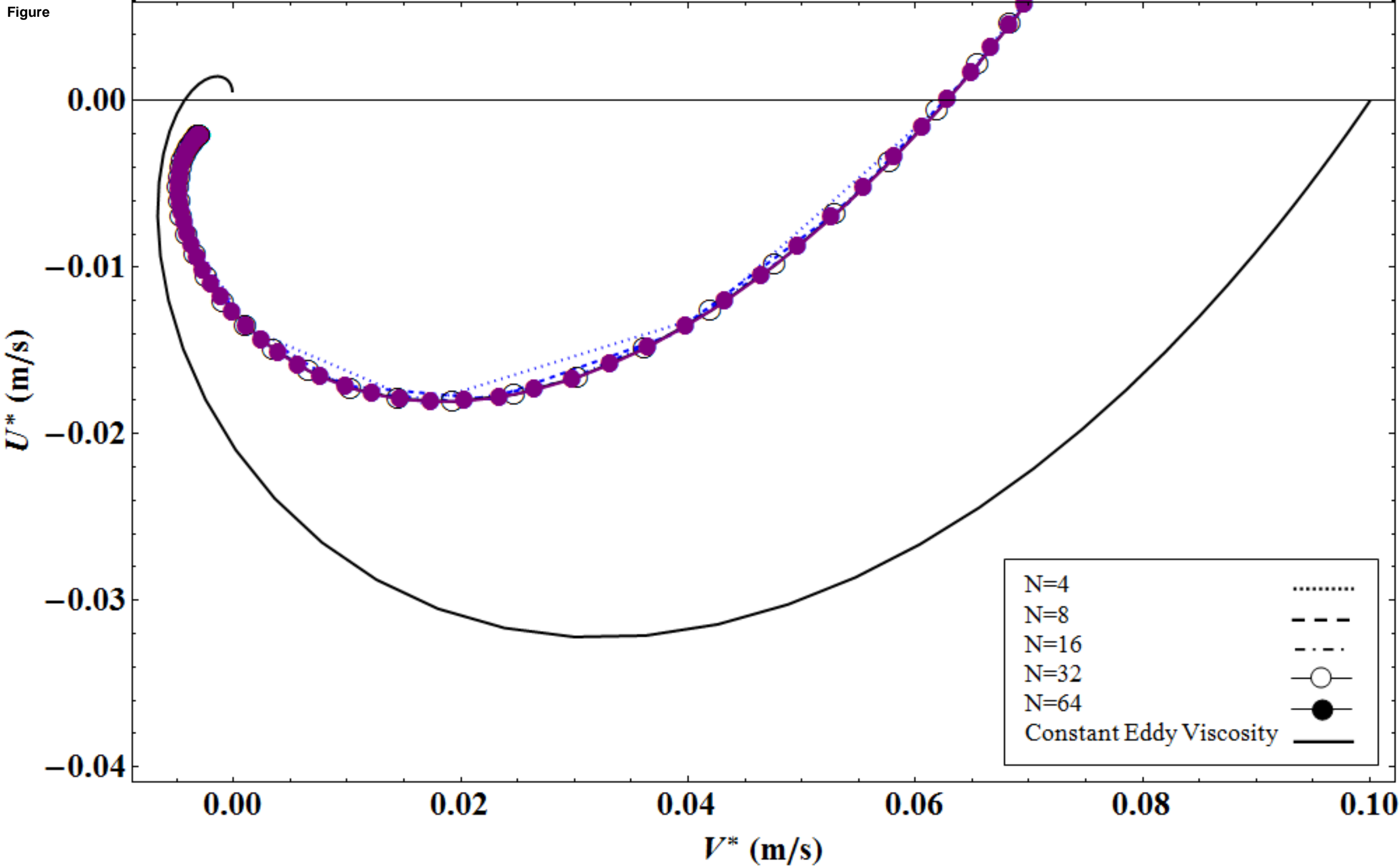
Figure

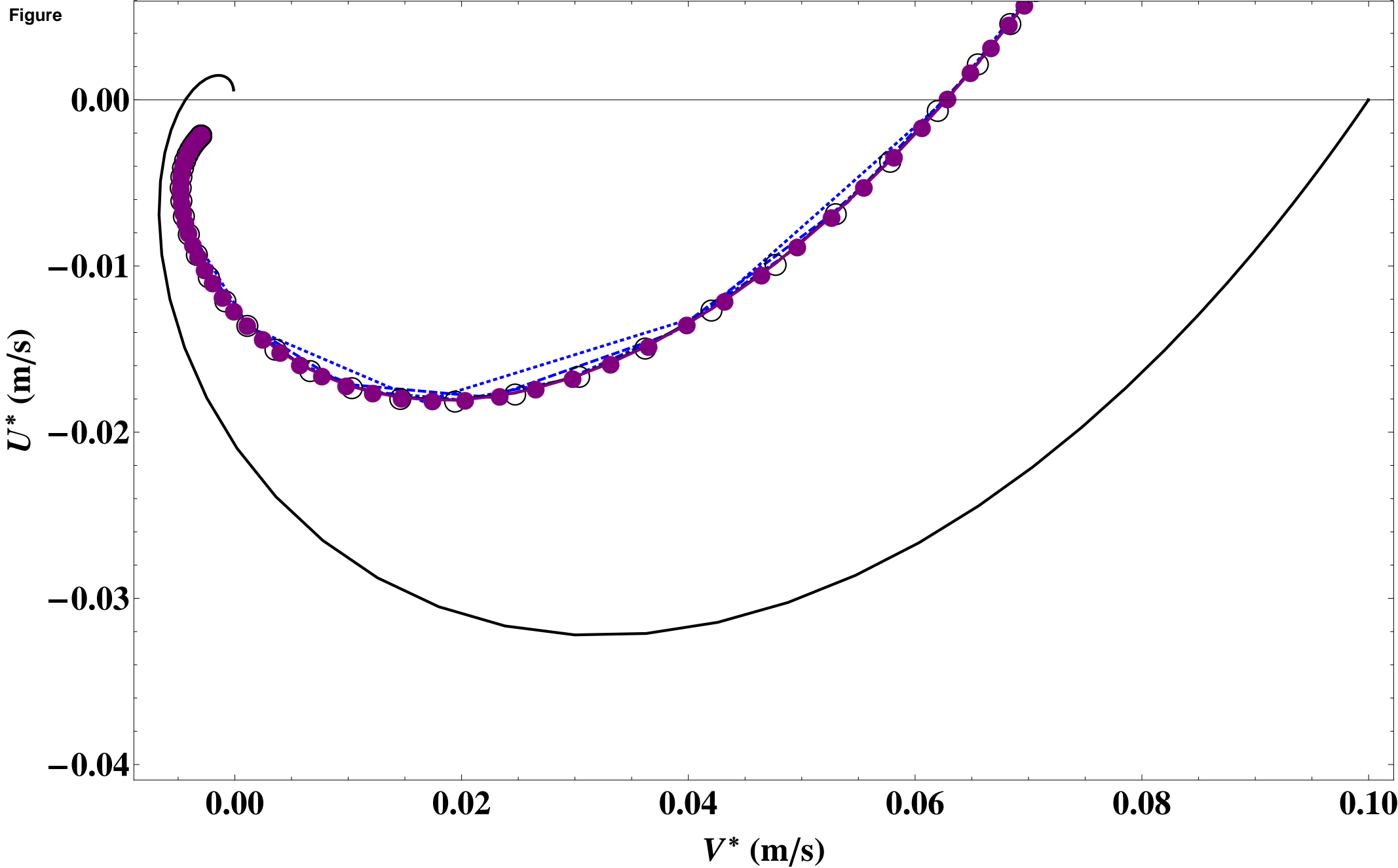


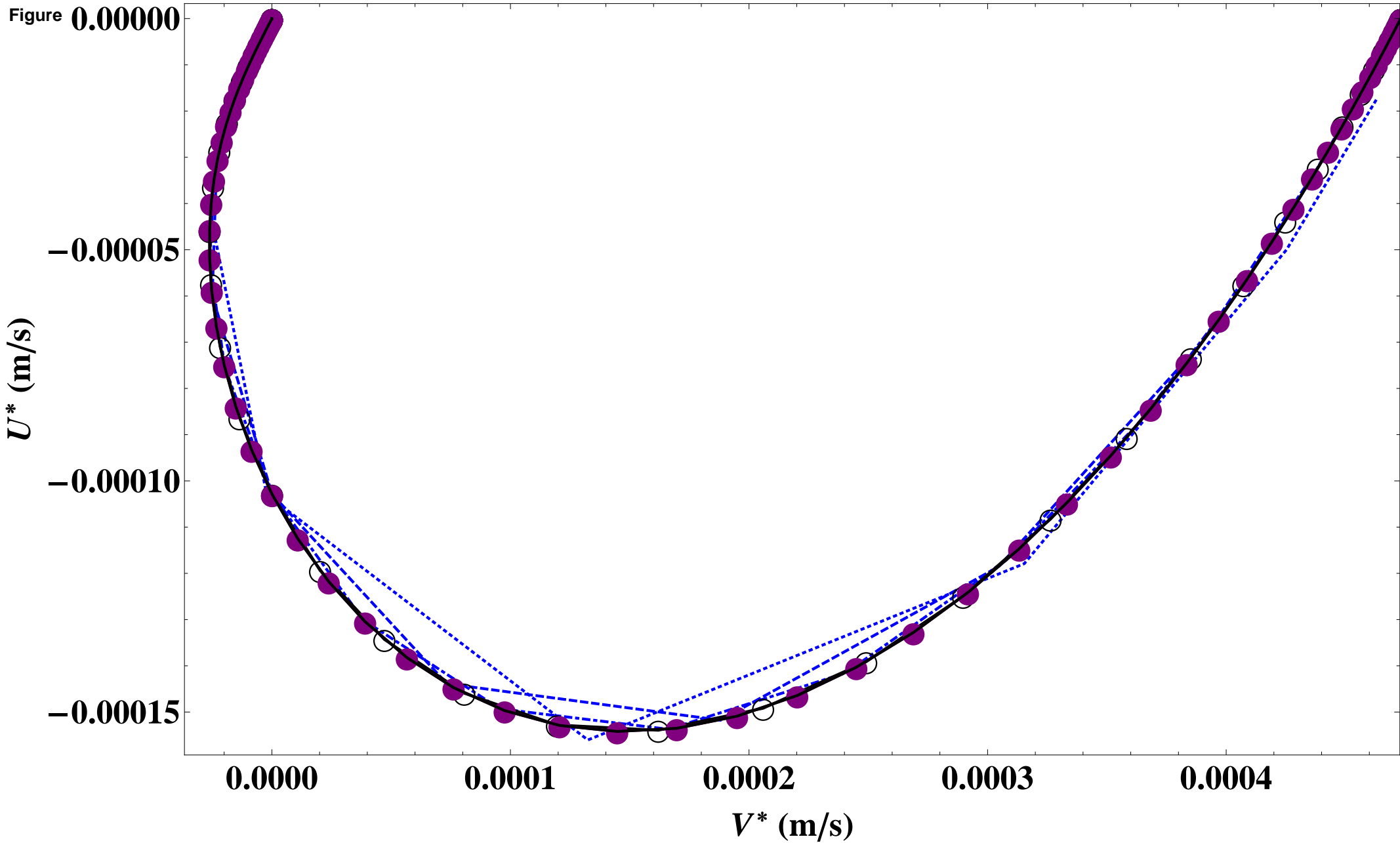
Figure



Figure







Figure

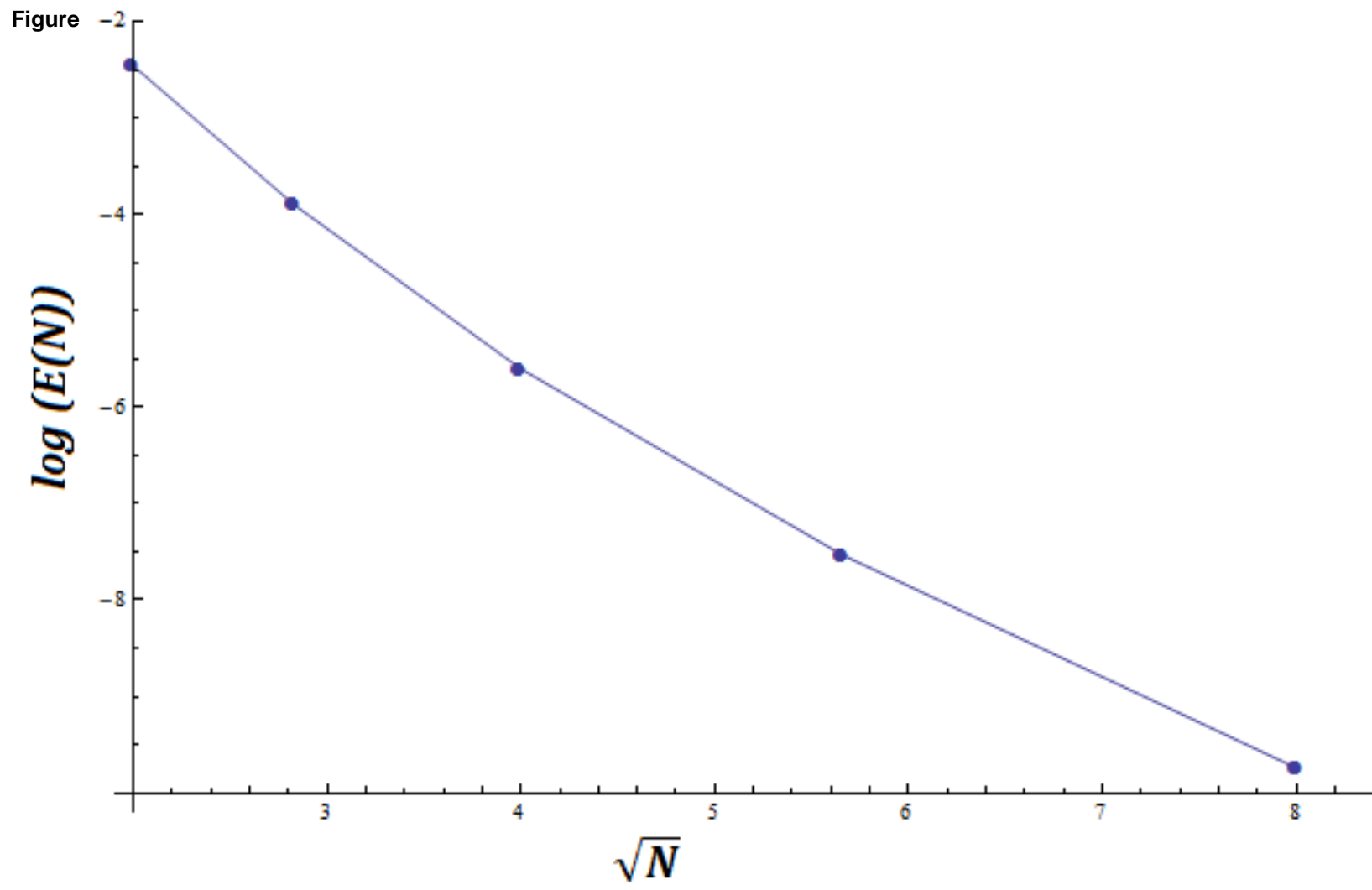


Figure 2

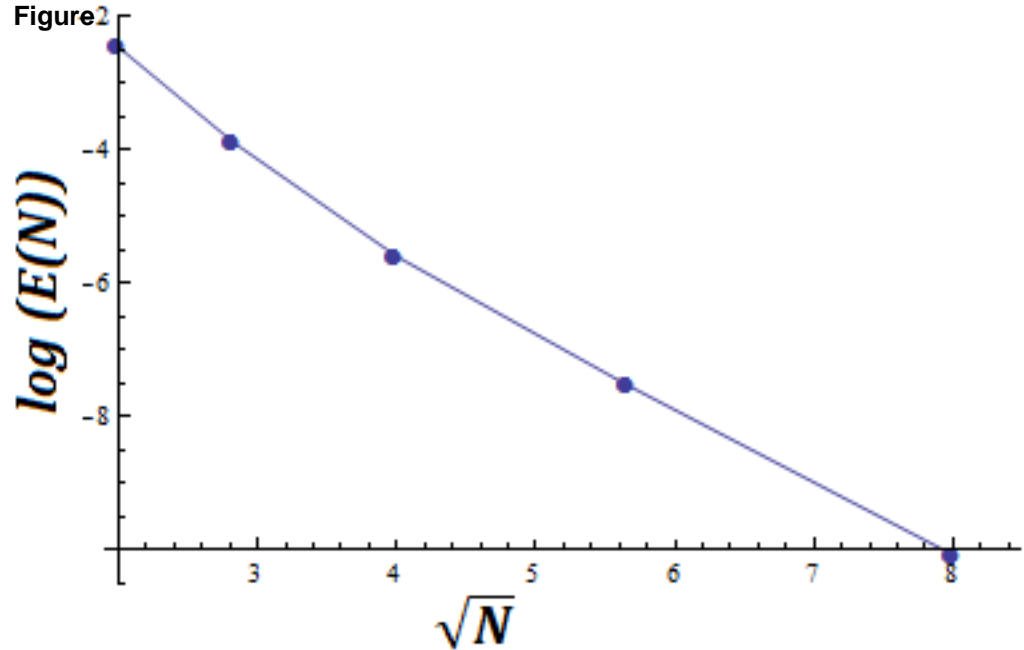


Figure 4

$\log(E(N))$

